DISEASE-CAUSING MUTATIONS IN HUMAN ENZYMES OF THE CDP-ETHANOLAMINE AND CDP-CHOLINE PATHWAYS CAUSE DISTINCT GROWTH AND PHOSPHOLIPID SYNTHESIS PHENOTYPES IN *SACCHAROMYCES CEREVISIAE*

by

Taryn M. Reid

Submitted in partial fulfilment of the requirements
for the degree of Master of Science

at

Dalhousie University
Halifax, Nova Scotia
August 2020

Dedication Page

This work is dedicated to my wonderful parents, Lisa and Bill. Thank you for always believing in me, for growing my love of learning, and for always being there to catch me when I fall. I appreciate and love you both so much.

TABLE OF CONTENTS

LIST OF TABLES ..... **vii**

LIST OF FIGURES ..... **viii**

ABSTRACT ..... **ix**

LIST OF ABBREVIATIONS USED ..... **x**

ACKNOWLEDGEMENTS ..... **xiii**

CHAPTER 1: INTRODUCTION **1**

1.1 Identification of Genetic Mutations Causing Rare Diseases **1**

1.2 Phosphatidylcholine in Eukaryotes **3**

1.2.1 Phosphatidylcholine Structure 4

1.2.2 Phosphatidylcholine Function 7

1.3 Phosphatidylethanolamine in Eukaryotes **8**

1.3.1 Phosphatidylethanolamine Structure 8

1.3.2 Phosphatidylethanolamine Function 8

1.4 Phosphatidylcholine Synthesis **10**

1.4.1 The CDP-choline Pathway 10

1.4.2 The Phosphatidylethanolamine Methylation Pathway 14

1.5 Phosphatidylethanolamine Synthesis via the CDP-ethanolamine pathway **16**

1.6 Phospholipid Synthesis in *Saccharomyces cerevisiae* **18**

1.7 Inherited Human Diseases Associated with Mutations in the CDP-Choline and CDP-Ethanolamine Pathways **20**

1.7.1 Spondylometaphyseal Dysplasia with Cone-rod Dystrophy 20

1.7.2 Leber Congenital Amaurosis 21

1.7.3 Congenital Lipodystrophy with Severe Fatty Liver Disease 22

1.7.4 Complex Hereditary Spastic Paraplegia 22

1.8 Objectives.....23

CHAPTER 2: MATERIALS AND METHODS 25

2.1 Materials 25

2.1.1 Plasmids and Primers 25

2.1.2 Yeast Strains 25

2.1.3 Antibodies 30

2.1.4 Restriction Enzymes 30

2.2 Protocols for Bacteria and Recombinant DNA Techniques 30

2.2.1 PCR and TOPO-TA Cloning 30

2.2.2 Site-directed Mutagenesis 33

2.2.3 Restriction Enzyme Digestion 34

2.2.4 Purification of DNA from Agarose Gel Using the GeneClean II Kit 34

2.2.5 Ligation Protocol with T4 DNA Ligase 35

2.2.6 Bacterial Transformation 36

2.2.7 Isolation of DNA from Transformed *Escherichia coli* Using the QIAPrep Spin Miniprep Kit 36

2.3 Microscopy 37

2.3.1 Fluorescence Microscopy 37

2.3.2 CCTα Localization Assay 38

2.4 Yeast Protocols 38

2.4.1 Yeast Transformation 38

2.4.2 Random Sporulation 39

2.4.3 Haploid Cell Selection 40

2.4.4 Serial Dilution Growth Assay 41

2.5 Techniques for Lipid Analysis 42

2.5.1 Metabolic Labeling of PE and Metabolites of the CDP-ethanolamine Pathway Using [^{14}C]Ethanolamine 42

2.5.2 Lipid Extraction 43

2.5.3 Lipid Phosphorus Determination 44

2.5.4 Thin-Layer Chromatography 44

2.6 Using SDS-Page and Western Blotting to Measure Protein Expression 45

CHAPTER 3: RESULTS 47

3.1 Human *PCYT1A* Can Replace *PCT1* Function in *Saccharomyces cerevisiae* 48

3.2 *PCYT1A* Translocates to Membranes in *Saccharomyces cerevisiae* in the Absence of Exogenous Choline 50

3.3 Generating the Disease-Causing Mutations in Human *PCYT1A* in *Saccharomyces cerevisiae* 52

3.4 Searching for Differential Phenotypes for *Saccharomyces cerevisiae* Transformed with *PCYT1A* Disease-causing Mutations when Exposed to Cell Stressors 56

3.5 Inositol and Reduced Choline Stress Result in Differential Phenotypes for *PCYT1A* Mutants 57

3.6 A Novel Patient-derived *EPT1* Mutation Reduces PE Synthesis via the CDP-Ethanolamine Pathway 62

CHAPTER 4: DISCUSSION 65

4.1 *PCYT1A* and Yeast Survival 66

4.2 *PCYT1A* Localization in Yeast 67

4.3 Mutations in *PCYT1A* Affect Yeast Growth.....68

4.3.1 *PCYT1A* E280del.....68

4.3.2 *PCYT1A* p.A93T.....70

4.3.3 *PCYT1A* p.A99T.....70

4.3.4 *PCYT1A* p.V142M.....71

4.4 The Effect of a Novel Patient-Derived *EPT1* Mutation on PE Synthesis.....72

CHAPTER 5: CONCLUSIONS AND FUTURE DIRECTIONS.....74

REFERENCES.....76

List of Tables

2.1 Plasmids Used in this Study 26

2.2 Plasmids Constructed for this Study 27

2.3 Yeast Strains Used in this Study 29

2.4 Antibodies Used in this Study 31

2.5 Restriction Enzymes Used in this Study 32

List of Figures

1.1 Structure of phosphatidylcholine 5

1.2 Models of PC demonstrating how fatty acyl chain length and degree of unsaturation can affect the shape of PC, which in turn affects membrane fluidity and thickness 6

1.3 Structure of phosphatidylethanolamine 9

1.4 The CDP-choline pathway in humans 11

1.5 The PE methylation pathway in humans 15

1.6 The CDP-ethanolamine pathway in humans 17

1.7 Pathways for PC and PE synthesis in yeast 19

3.1 Supplementation with exogenous choline allows growth and survival of haploid yeast cells that are expressing human *PCYT1A* and lack the PE methylation pathway 51

3.2 Fluorescence microscopy depicting the localization of human PCYT1A in the presence and absence of choline 53

3.3 Protein map of human PCYT1A denoting the domains and the identified mutations that cause inherited human diseases 54

3.4 Growth analysis of haploid yeast cells transformed with human *PCYT1A* and the disease-causing mutant variants at 30 °C with 200 μM or 5 μM choline 58

3.5 Growth analysis of haploid yeast cells transformed with human *PCYT1A* and the disease-causing mutant variants of the gene grown in the presence of 0.01% sodium dodecyl sulphate, 200 μM or 0.5 μM choline, and 11 μM inositol 60

3.6 Growth analysis of haploid yeast cells transformed with human *PCYT1A* and the disease-causing mutant variants of the gene grown in the presence of 50 μM Cd^{2+}, 200 μM or 0.5 μM choline, and 11 μM inositol 61

3.7 The effect of the patient-derived P45L mutation on human EPT1 activity 64

Abstract

Phosphatidylcholine and phosphatidylethanolamine are two of the most abundant phospholipids present in eukaryotic cells. In mammalian cells, these are mainly synthesized through the Kennedy pathways. *PCYT1A* is the gene that codes for the rate-limiting step in the CDP-choline pathway. Three rare inherited diseases have been associated with mutations in this gene. *EPT1* is the gene that codes for the final step in the CDP-ethanolamine pathway and new patient-derived mutation has been associated with complex hereditary spastic paraplegia. I sought to better understand how these mutations affect the protein function using yeast as a model organism. Using serial dilution pinning assays, I discovered that some of the mutations in *PCYT1A* cause altered growth compared to the wild type when exposed to certain cell stressors. By studying the novel patient-derived mutation in *EPT1* using metabolic radiolabelling of the CDP-ethanolamine pathway, I determined that this mutation causes a decrease in enzyme activity.

List of Abbreviations Used

ADP	Adenosine diphosphate
APS	Ammonium persulphate
ATP	Adenosine triphosphate
CCT	CTP:phosphocholine cytidylyltransferase
Cd^{2+}	Cadmium
CDP	Cytidine diphosphate
CEPT	Choline/ethanolamine phosphotransferase
CHK	Choline kinase
CHT	Choline transporter
CL-FLD	Congenital lipodystrophy with severe fatty liver disease
CLT	Choline-like transporter
CMP	Cytidine monophosphate
CPT	Cholinephosphotransferase
CTP	Cytidine triphosphate
DAG	Diacylglycerol
DIC	Differential interference contrast
DNA	Deoxyribonucleic acid
dNTP	Deoxynucleoside triphosphate
ECT	CTP:phosphoethanolamine cytidylyltransferase
EK	Ethanolamine kinase
EPT	Ethanolaminephosphotransferase
ER	Endoplasmic reticulum

G418	Geneticin
GFP	Green fluorescent protein
HDL	High density lipoprotein
HIS	Histidine
HSP	Hereditary spastic paraplegia
HYG	Hygromycin B
KAN	Kanamycin
LB	Lysogeny broth
LCA	Leber congenital amaurosis
LCAT	Lecithin-cholesterol acyltransferase
LEU	Leucine
LiAc	Lithium acetate
LYS	Lysine
MET	Methionine
NGS	Next-generation sequencing
OCT	Organic cation transporter
OD	Optical density
ORF	Open reading frame
PC	Phosphatidylcholine
PCR	Polymerase chain reaction
PE	Phosphatidylethanolamine
PEG	Polyethylene glycol
PEMT	Phosphatidylethanolamine N-methytransferase

PPAR	Peroxisome proliferator activator receptor
PPi	Pyrophosphate
RCT	Reverse cholesterol transport
RER	Rough endoplasmic reticulum
Rpm	Revolutions per minute
SAH	S-Adenosyl homocysteine
SAM	S-Adenosyl methionine
S. cerevisiae	*Saccharomyces cerevisiae*
SDS	Sodium dodecyl sulphate
SC	Synthetic complete
SM	Minimal media
SMD-CRD	Spondylometaphyseal dysplasia with cone-rod dystrophy
SNV	Single-nucleotide variant
TAE	Tris-acetate-EDTA
TE	Tris-EDTA
TLC	Thin-layer chromatography
URA	Uracil
UV	Ultraviolet
V	Volt
VLDL	Very low-density lipoprotein
WES	Whole-exome sequencing
WGS	Whole-genome sequencing
YPD	Yeast extract-peptone-dextrose

Acknowledgements

I would like to say a huge thank-you to Dr. Christopher McMaster. His unwavering support and kindness helped to make my program an amazing experience. I would also like to thank him for creating such a welcoming and supportive lab environment that really allows graduate students to learn and grow.

I would also like to say thank-you to Dr. Pedro Fernandez-Murray. I am thankful that he was always there to help me problem-solve and provide great constructive criticism, and that he was always a friendly face to chat with (especially about gardening!). I am so grateful that Pedro was there to mentor me throughout my Masters and without him this experience would not have been nearly as enjoyable.

Also, I would like to say thank-you to Dr. Mahtab Tavasoli for being such a great friend in the lab and for being my first mentor in academia. Her kindness and patience with me while I was learning all new techniques is greatly appreciated. I'm also thankful that she was always a friend that I could go talk to about anything (be it science or life related).

I would like to say a special thank-you to Sarah and Katherine for being such great friends throughout my program. You've made this Masters such an incredible experience for me and I'm so thankful to be able to call you my friends.

Thank-you to Jason Williams, Dr. Pedro Fernandez-Murray, and Maren Brodovsky for their help with the work involving EPT1.

Lastly, I would like to thank the rest of the McMaster lab, the ARC, and my committee (Dr. Christopher Sinal and Dr. James Fawcett) for being so helpful and kind over the last few years. Thank you for all that you've taught me.

CHAPTER 1: INTRODUCTION

1.1 Identification of Genetic Mutations Causing Rare Diseases

Rare diseases (often referred to as orphan diseases) are defined as diseases that affect less than 1 in 2000 people[1]. Although the individual diseases are rare, rare diseases as a whole are actually quite common and affect millions of individuals worldwide. To date, there have been over 8000 distinct rare disease traits that have been identified[2]. Most rare diseases are inherited and it is estimated that at any point in time, there is a prevalence of 3.5-5.9% for rare diseases in the global population[87]. Inherited diseases are often caused by genetic abnormalities consisting of rare single nucleotide variants, insertion or deletion variants, and copy number variants[2]. Thus far, the molecular aetiologies of ~5000 inherited diseases have been determined. Many inherited diseases present early in childhood and unfortunately, 30% of children with an inherited disease will pass away in their first year of life[3]. Therefore, it is incredibly important that researchers study inherited diseases to attempt to provide treatment options and information for families and to alleviate some of the strain that these conditions cause on society and the healthcare system.

Information on inherited diseases is rapidly becoming more available. Much of this has to do with the declining cost of sequencing a human genome. The Human Genome Project was completed in 2003 and took over ten years to finish at a cost of more than $1 billion. Today, a human genome can be sequenced for less than $1000 and in one day[4]. The significant decrease in cost is allowing genetic/genomic testing to be performed far more frequently. This has lead to a substantive increase in the identification of human gene variants that cause inherited diseases.

Much of the early identification of rare disease-causing genes was done through linkage mapping and candidate gene analysis, but the introduction of next-generation sequencing (NGS) allowed researchers to accelerate the discovery process[1]. Today, the most widely used screening techniques are whole-genome sequencing (WGS) and whole exome sequencing (WES), where only the protein-coding portion of the genome (1.5%) is sequenced. Results are analyzed against genomic databases to distinguish the disease-causing genetic variations from variants that commonly occur in the population[1]. Disease-causing genetic mutations can be inherited or can occur *de novo*. On average, there are approximately 74 single-nucleotide variants (SNVs) that occur per genome per generation, though not all of these variations are associated with disease[5]. WES and WGS have proven to be great tools in identifying not only if a genetic variation appears to be disease causing, but also in aiding to determine if a genetic mutation is occurring *de novo*.

There exist many different strategies to study rare diseases and the strategy chosen is often related to the mode of inheritance of the disease. In the presence of consanguinity or familial recurrence of a rare disease phenotype, the likelihood that the disease is monogenic is high[1]. In the case of autosomal recessive diseases where there does not appear to be consanguinity, mutations are often compound heterozygous meaning that a different mutant allele is present on each copy of the gene. When consanguinity is observed, homozygous mutations are anticipated. In both of these instances, immediate family (siblings and parents) can be screened for gene variants. In the case of autosomal dominant disorders, analysis of a large pedigree may be required to

determine the gene involved. In *de novo* genetic mutations, WES from a trio of parents and patients will normally yield a candidate gene[1].

For my study, I looked at rare inherited diseases caused by genetic variations in two genes in the Kennedy pathways, *PCYT1A* and *EPT1*. *PCYT1A* encodes the enzyme that catalyzes the rate-determining step in the synthesis of the phospholipid phosphatidylcholine (PC), while *EPT1* codes for the enzyme that catalyzes the terminal step in the Kennedy pathway for the synthesis of phosphatidylethanolamine (PE). Autosomal recessive mutations in human *PCYT1A* have been associated with three rare diseases: spondylometaphyseal dysplasia with cone-rod dystrophy, Leber congenital amaurosis, and congenital lipodystrophy with severe fatty liver disease. Autosomal recessive mutations in human *EPT1* are associated with complex hereditary spastic paraplegia.

1.2 Phosphatidylcholine in Eukaryotes

Phospholipids are an essential component of biological membranes. These membranes are necessary for many functions that ensure cell survival such as protection from the environment, segregation and compartmentalization of specific cellular functions into organelles, vesicular trafficking between organelles, and cell signalling[6]. The lipid composition of membranes can also influence fluidity[7]. PC is the most abundant phospholipid present in eukaryotic cell membranes[8]. This essential phospholipid makes up ~50% of the total phospholipid mass in most eukaryotic cell types[9].

1.2.1 Phosphatidylcholine Structure

The PC molecular structure consists of a glycerol backbone with two fatty acid chains and a phosphocholine moiety (Figure 1.1). The fatty acid chains can range from 14-26 carbons in length, but most PC species contain chains of 16 or 18 carbons[9]. The length of the chains can influence membrane fluidity and packing of the membranes with longer chains providing a less fluid membrane. The number of double bonds present in fatty acid chains can also influence the fluidity of membranes. Saturated fatty acid chains and monounsaturated fatty acid chains have been found to be less fluid than polyunsaturated fatty acid chains[10]. This is because the introduction of double bonds does not allow for tight membrane packing because of the kinks in the chains that are formed due to fatty acid unsaturation (Figure 1.2). Not all PC molecules have the same function and this has been shown by PC species with specific chain lengths and saturation properties being used for specific biological roles. An example of different PC species being used for a specific function is in the synthesis of lung surfactant (a substance secreted by type II alveolar cells to reduce surface tension and prevent collapsing of the lungs upon exhalation) where the PC composition is approximately 60% 16:0/16:0-PC, 30% 16:0/16:1-PC, and 10% 16:0/14:0-PC[11]. Slightly different PC species are also synthesized depending on whether the PC was made through the CDP-choline pathway or the PE methylation pathway, with longer chain unsaturated PC species being synthesized by the latter and medium chain saturated species being produced by the former[12].

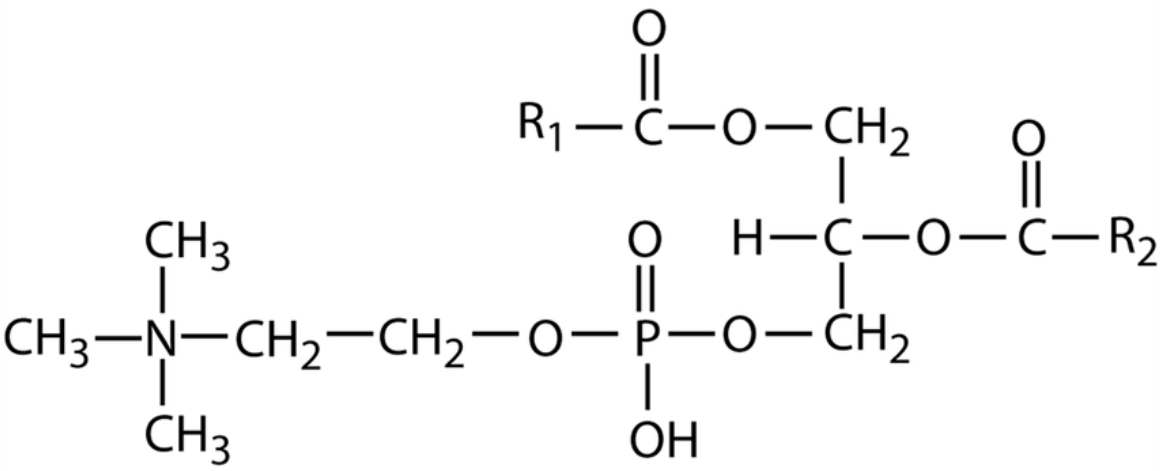

Figure 1.1: **Structure of phosphatidylcholine.** Structure consists of a glycerol backbone, two fatty acyl chains, and a choline headgroup. R_1 and R_2 represent the fatty acyl chains.

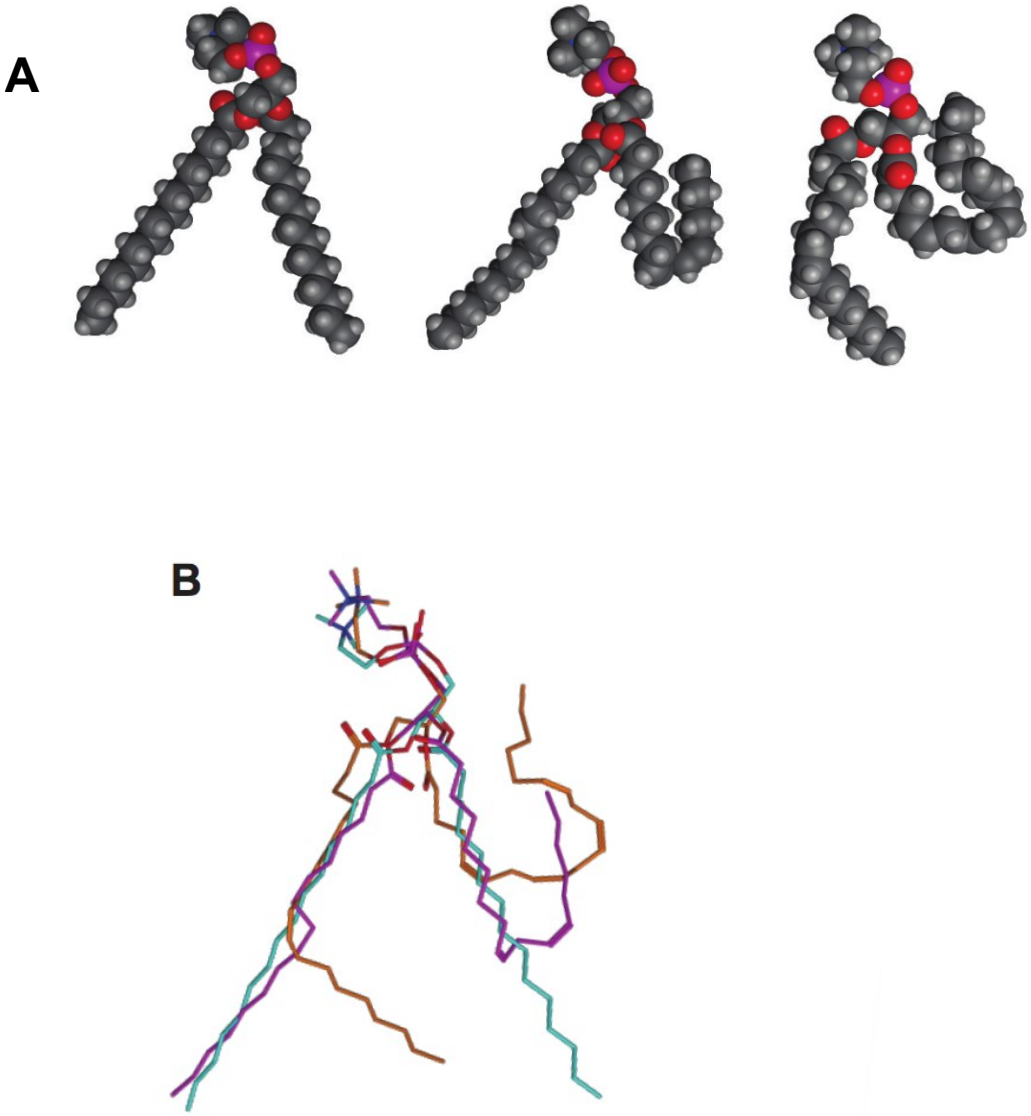

Figure 1.2**: Models of PC demonstrating how fatty acyl chain length and degree of unsaturation can affect the shape of PC, which in turn affects membrane fluidity and thickness**. *A.* Space fill models of 16:0/16:0-PC; 16:0/18:2-PC, and 18:1/20:4-PC. Carbon atoms are dark grey, hydrogen atoms are light grey, oxygen atoms are red, and phosphorus atoms are purple.
B. Overlap line drawing of 16:0/16:0-PC (cyan); 16:0/18:2-PC (purple), and 18:1/20:4-PC (orange) illustrate the different shapes of the PC species with differing fatty acyl chains[9].

1.2.2 Phosphatidylcholine Function

PC serves many different functions in cells and this is not surprising given the universal presence of the CDP-choline pathway in eukaryotic cells. It is especially important in the formation of cellular membranes. The lipid bilayer structure that is present in cells is important for separating the interior contents of the cell from the aqueous exterior environment. This bilayer is also semi-permeable to allow for transport of necessary materials into the cell. The long fatty acid tails point inwards to form a hydrophobic core while the choline headgroups point outwards towards the aqueous environment inside and outside of the cell.

PC has many other functions in humans outside of membrane formation. As mentioned previously, different PC species play an important role in the synthesis of lung surfactant. Some other examples include PC having roles in reverse cholesterol transport (RCT), very low density lipoprotein (VLDL) secretion from the liver, and as a substrate for peroxisome proliferator activator receptors (PPARs).

RCT is an important process that is used to transport excess cholesterol from peripheral tissues and transport them to the liver for excretion[13]. The transportation of cholesterol happens by high density lipoproteins (HDLs) and PC is important in this process as it is present on the surface of lipoproteins and is the key binding component of HDLs to cholesterol[14]. PC also functions as the substrate for lecithin-cholesterol acyltransferase (LCAT) to produce cholesterol esters[15].

PC is an important part of VLDL assembly and secretion from the liver. VLDL is responsible for transporting hepatic fatty acids for storage in fat deposits[16]. PC coats the

VLDL and an increase in PC synthesis can influence the production of VLDL. Not only that, but PC species with polyunsaturated fatty acid chains at the *sn-2* position can cause increased membrane fluidity and in turn, create a more suitable environment for apoB to get incorporated into VLDL[17].

Lastly, 16:0/18:1-PC has been found to be an endogenous ligand for PPARα[18]. PPARs are nuclear receptor proteins that play a role in regulating gene expression. The binding of this PC species to PPARα leads to the expression of many genes involved in lipid metabolism[18].

1.3 Phosphatidylethanolamine in Eukaryotes

1.3.1 Phosphatidylethanolamine Structure

The structure of PE consists of a glycerol backbone with two long fatty acid chains and an ethanolamine headgroup (Figure 1.3). Like PC, different species of PE (characterized by differing fatty acid chain lengths and the number of double bonds) can have an effect of the fluidity and packing of cell membranes[19].

1.3.2 Phosphatidylethanolamine Function

PE is another essential phospholipid in mammalian cells and it is the second most abundant after PC. It makes up ~25% of all mammalian phospholipids across most cell types, but it is especially important in the brain where 45% of phospholipid content is PE[20]. Like PC, PE is heavily involved in the formation of cellular membranes. Due to its ability to form an inverted hexagonal phase structure, via its small head group versus the

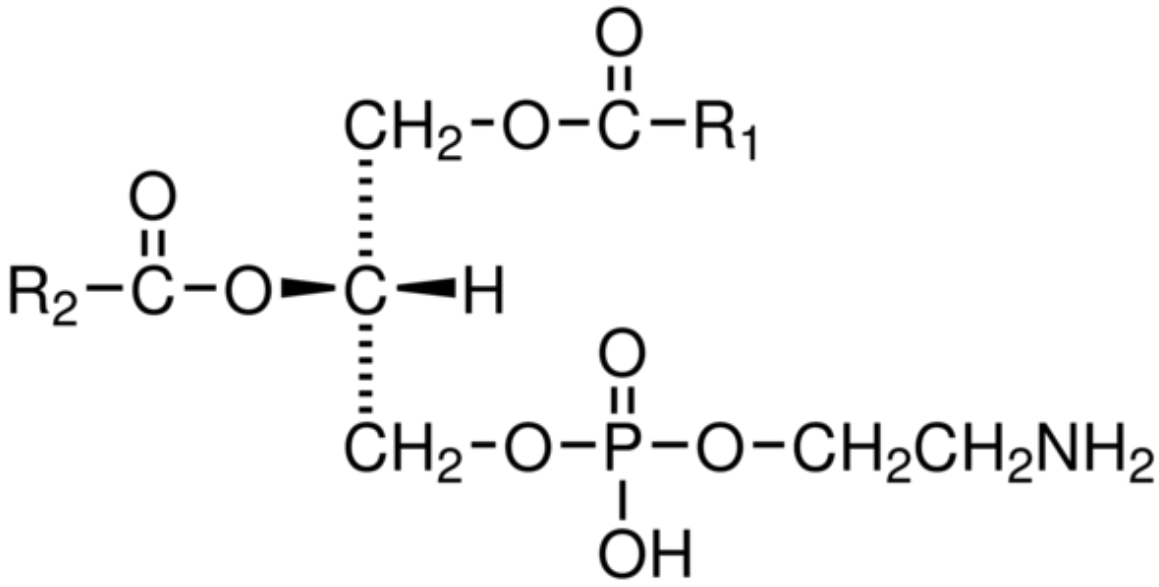

Figure 1.3: **Structure of phosphatidylethanolamine.** Structure consists of a glycerol backbone, two fatty acyl chains, and an ethanolamine headgroup. R_1 and R_2 represent the fatty acyl chains.

width of its fatty acyl chains, PE has also been implicated in membrane fusion and fission during endocytosis, exocytosis, cytokinesis, and vesicle trafficking[21, 22].

1.4 Phosphatidylcholine synthesis

PC can be synthesized through two different pathways in eukaryotes. The first, and most abundantly used pathway for PC synthesis in human cells, is the Kennedy pathway (CDP-choline pathway). The second method that some eukaryotic cells (yeast and mammalian hepatocytes) use for PC synthesis is the conversion of PE to PC through the PE methylation pathway.

1.4.1 The CDP-choline Pathway

The CDP-choline pathway (Figure 1.4) is a three-step pathway that converts choline to PC. Choline is an essential nutrient that mammals must consume through their diet to maintain normal physiological function, as it is required for the biosynthesis of PC[23]. Since choline is a molecule that possesses a positive charge, it is unable to freely cross the membrane on its own and requires a transporter to enter the cell[24]. In humans, three classes of proteins responsible for choline transport have been identified: the high-affinity choline transporters (CHTs) in neuronal cells, the low-affinity organic cation transporters (OCTs), and the intermediate-affinity choline-like transporters (CLTs)[25, 26]. The CLT1 transport protein has been proposed to be the main transporter for choline that gets used for PC synthesis[27, 28].

The first step in the CDP-choline pathway involves the phosphorylation of choline to produce phosphocholine catalyzed by choline kinase and with the donation of

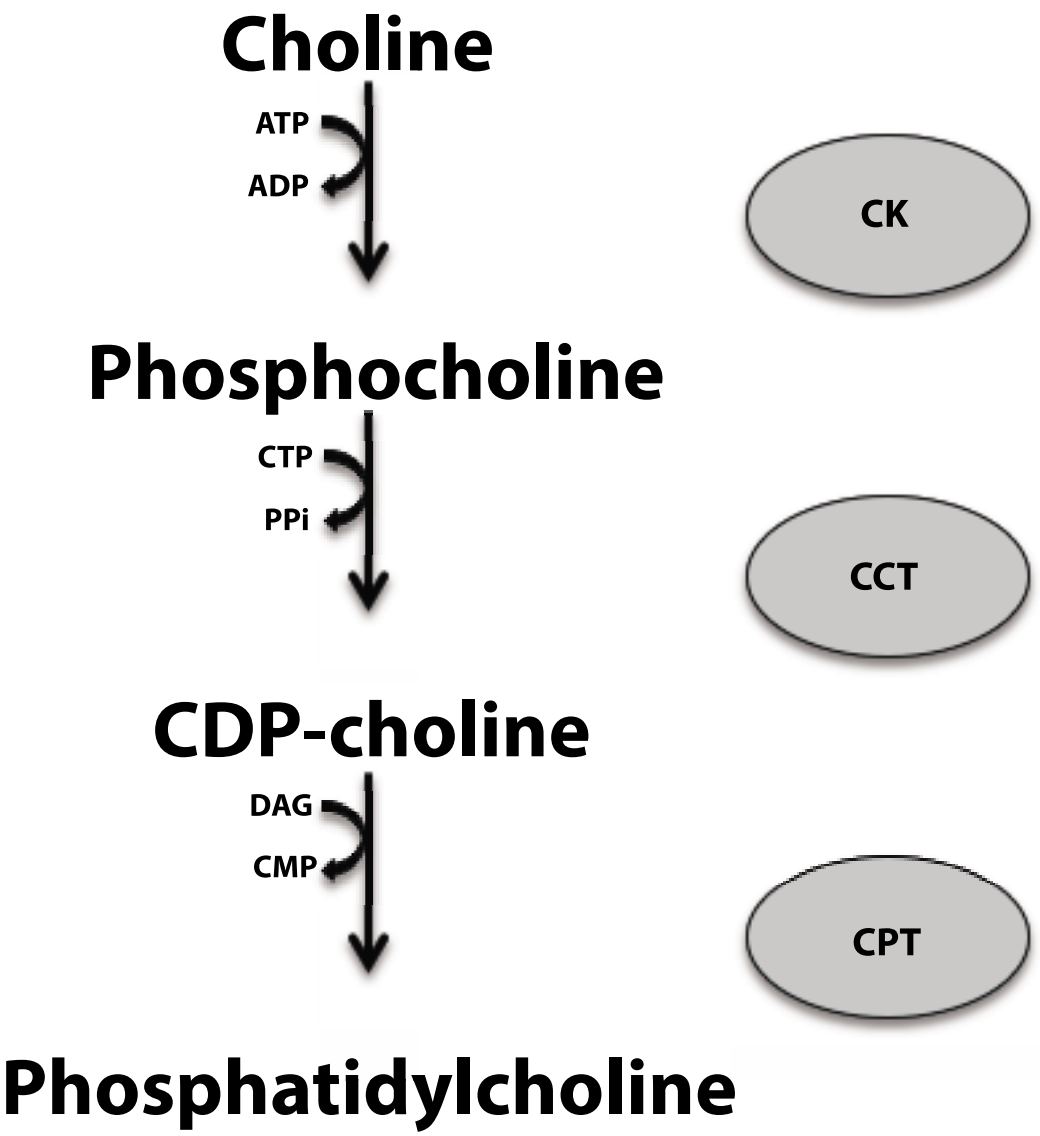

Figure 1.4: **The CDP-choline Pathway in Humans.** Choline gets converted to phosphocholine while adenosine triphosphate (ATP) gets converted to adenosine diphosphate (ADP) by choline kinase (CK). Phosphocholine gets converted to CDP-choline by CTP:phosphocholine cytidylyltransferase (CCT) with the addition of cytidine triphosphate (CTP) that gets changed to pyrophosphate (PPi). Lastly, CDP-choline gets converted to phosphatidylcholine by cholinephosphotransferase (CPT) with the addition of diacylglycerol (DAG) and the release of cytidine monophosphate (CMP).

the phosphate group by ATP[29]. Humans possess two genes (*CHKA* and *CHKB)* that code for 3 different choline kinase isoforms: CHKα1, CHKα2, and CHKβ[30]. Choline kinases are soluble proteins that are found in the cytoplasm[9]. Knocking out *Chka* in mice has been shown to be embryonic lethal, but mice that were heterozygous for *Chka* did not show a noticeable phenotype (although they were unable to produce PC as efficiently as wild type mice)[31]. When *Chkb* is knocked out in mice, a form of rostrocaudal muscular dystrophy and bone deformations occur[32]. When loss-of-function mutations are present in human *CHKB*, this form of congenital muscular dystrophy is recapitulated[33, 34]. Interestingly, an increase in choline kinase activity is seen in breast, lung, colorectal, and prostate cancers, which leads to the possibility of using choline kinase as a tumour marker[35].

The second, and rate-determining, step of the CDP-choline pathway is the conversion of phosphocholine and cytidine triphosphate (CTP) to CDP-choline and pyrophosphate catalyzed by CTP:phosphocholine cytidylyltransferase (CCT) [9]. In mammals CCT protein can be produced by two separate genes, *PCYT1A* and *PCYT1B*, which code for CCTα and CCTβ, respectively. *PCYT1A* is universally expressed while *PCYT1B* is mostly expressed in the brain and reproductive tissues[36]. CCTα is the most studied of the isoforms. CCTα consists of membrane-bound and soluble forms that localize mainly to the nuclear envelope/ER when catalytically active and localize to the nucleoplasm when inactive[37]. There is also evidence in some cell types (such as rat liver cells) that CCTα can also localize to the cytoplasm when inactive[38].

Human CCTα is a 367 amino-acid residue protein that contains four functional domains: an N-terminal domain containing the nuclear localization signal, a catalytic

domain, a membrane-binding domain, and a C-terminal phosphorylation domain[39]. There is evidence that the amphipathic helix present in the membrane-binding domain is responsible for activation of the enzyme[40]. Studies from the Cornell lab have uncovered that CCT homodimerizes[41]. They have also determined how the enzyme is regulated. When the enzyme is inactive, the amphipathic helix of each monomer folds up and forms a complex of four helices with two helices of the catalytic domain[42]. This complex changes the conformational shape of the enzyme and prevents access to essential catalytic residues in the catalytic core. When the enzyme binds to a membrane, the helices of the membrane-binding domain are displaced and become embedded in the membrane surface. This allows the required conformational changes to occur and also enables substrates to access the catalytic core[42]. This process is selective for membranes that have high negative surface change and loose packing, ensuring that the enzyme is only catalytically active when the cell requires PC synthesis[43].

Both α and β isoforms of CCT are important for normal mammalian health and development. When *Pcyt1a* knockout mice were studied, the absence of *Pcyt1a* resulted in early embryonic death and the zygotes did not develop past day 3.5[44]. Inactivation of the *Pcyt1b* gene in mice has an effect on the reproductive tissues with gonadal degeneration and reproductive deficiency occurring[45]. So while both isoforms are important, *Pcyt1b* is unable to compensate for a complete lack of *Pcyt1a* while *Pcyt1a* is able to somewhat compensate for a complete lack of *Pcyt1b* in mice. In humans, many disease-associated mutant variants of *PCYT1A* have been discovered. The mutations span the catalytic, membrane-binding, and phosphorylation domains and have been associated

with spondylometaphyseal dysplasia with cone-rod dystrophy, Leber congenital amaurosis, and congenital lipodystrophy with severe fatty liver disease[46-49].

The third and final step in the CDP-choline pathway involves the conversion of diacylglycerol (DAG) and CDP-choline to cytidine monophosphate (CMP) and PC catalyzed by cholinephosphotransferase (CPT1/CEPT1)[50]. CPT1 is specific for CDP-choline as a substrate and synthesizes PC exclusively, while CEPT1 is able to catalyze reactions with both CDP-choline and CDP-ethanolamine resulting in the synthesis of both PC and PE[51]. CPT1 is an integral membrane protein that is associated with the Golgi apparatus while CEPT1 is present in the endoplasmic reticulum[52]. Though no genetic diseases have been associated with CPT1 or CEPT1, a muscle-specific *Cept1* knockout mouse was generated, and when fed a high-fat diet they showed increased insulin sensitivity and exercise intolerance[53].

1.4.2 The Phosphatidylethanolamine Methylation Pathway

In humans, the PE methylation pathway (Figure 1.5) is not as abundantly used for PC synthesis as the CDP-choline pathway as it only occurs in hepatocytes and accounts for about 30% of hepatic PC production[54]. The reaction starts with PE and in three successive methylations of the molecule with S-adenosyl methionine (SAM) by phosphatidylethanolamine N-methyltransferase (PEMT) the resulting product, PC, is synthesized[55]. PEMT is localized to the endoplasmic reticulum and is enriched at endoplasmic reticulum-mitochondrial-associated membranes. It has been shown in a diabetic mouse model that inhibition of *Pemt* reduces ER stress associated with diabetic

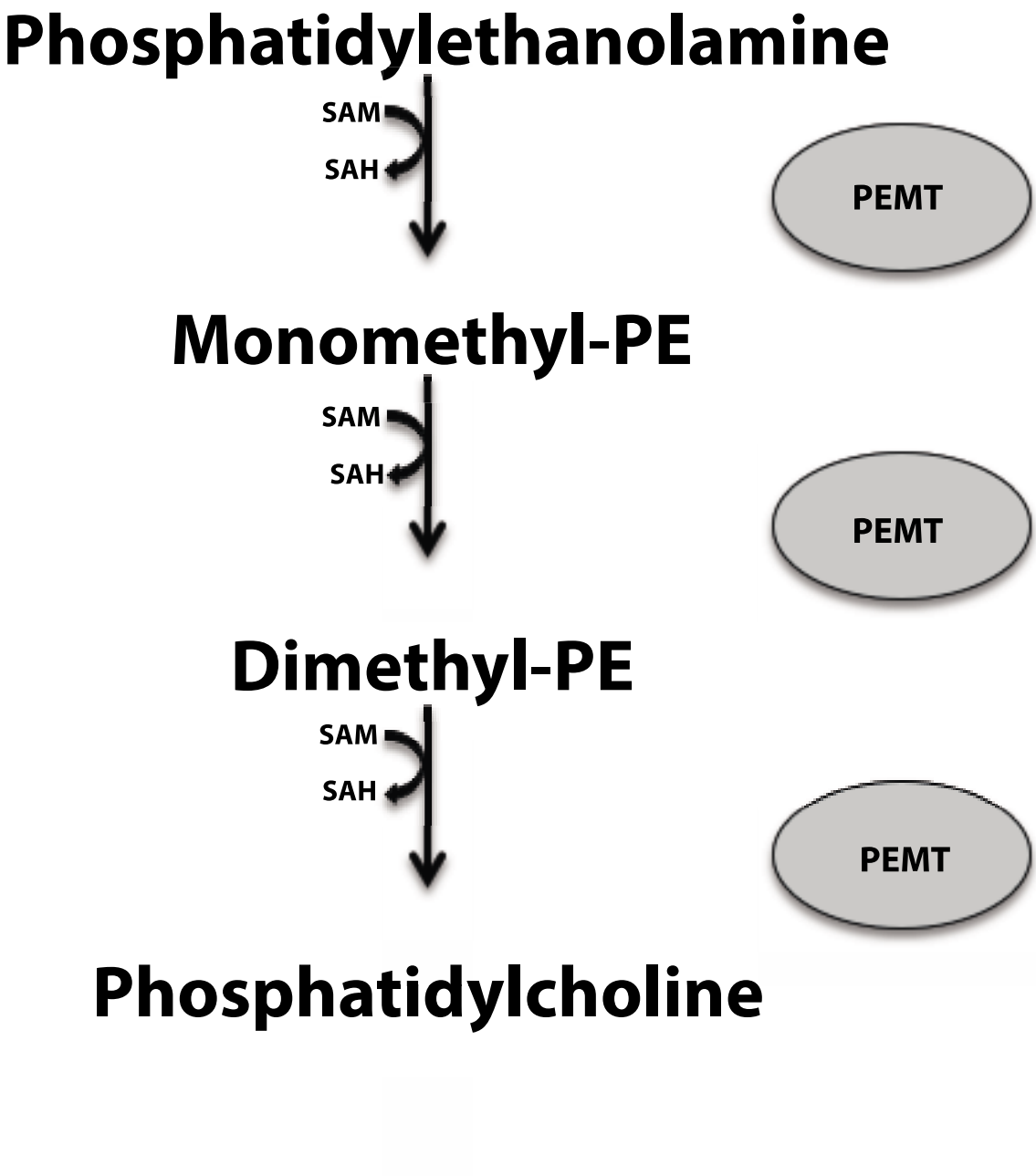

Figure 1.5: **The PE methylation pathway in humans.** Phosphatidylethanolamine gets converted to phosphatidylcholine by three successive methylations catalyzed by phosphatidylethanolamine N-methyltransferase (PEMT) with the addition of S-Adenosyl methionine (SAM) that gets converted to S-Adenosyl homocysteine (SAH).

neuropathy[56]. In mice, it has also been shown that the PE methylation pathway is nonessential for survival as mice that were homozygous for *Pempt* disruption showed no adverse phenotypes and the CDP-choline pathway was able to compensate for a lack of PC synthesis from the PE methylation pathway[57].

1.5 Phosphatidylethanolamine Synthesis via the CDP-ethanolamine Pathway

The CDP-ethanolamine pathway (Figure 1.6) is a three-step pathway that converts ethanolamine to PE. Ethanolamine transport has shown to be Na^+-dependent which means that it is likely being transported across the cell membrane by a different mechanism than choline[58]. The ethanolamine transporter has yet to be identified.

The first step in the CDP-ethanolamine pathway is the conversion of ethanolamine and ATP to phosphoethanolamine and ADP by ethanolamine kinase (EK). EK has been proposed to be rate limiting for the CDP-ethanolamine pathway, but experimental results have been mixed[59-61]. Two genes code for EK in humans, *ETNK1* codes for EK1 and *ETNK2* codes for EK2. EK1 and EK2 have been purified and EK1 has ethanolamine kinase activity and no choline kinase activity, while EK2 has ethanolamine kinase activity and a low level of choline kinase activity[62]. An autosomal recessive missense mutation in *EK1* has been linked to systemic mastocytosis, which is characterized by the accumulation of mast cells in extra-cutaneous organs[63].

The second step of the CDP-ethanolamine pathway involves the conversion of phosphoethanolamine and CTP to CDP-ethanolamine and pyrophosphate (PPi) catalyzed by CTP:phosphoethanolamine cytidylyltransferase (ECT). ECT is encoded by a single

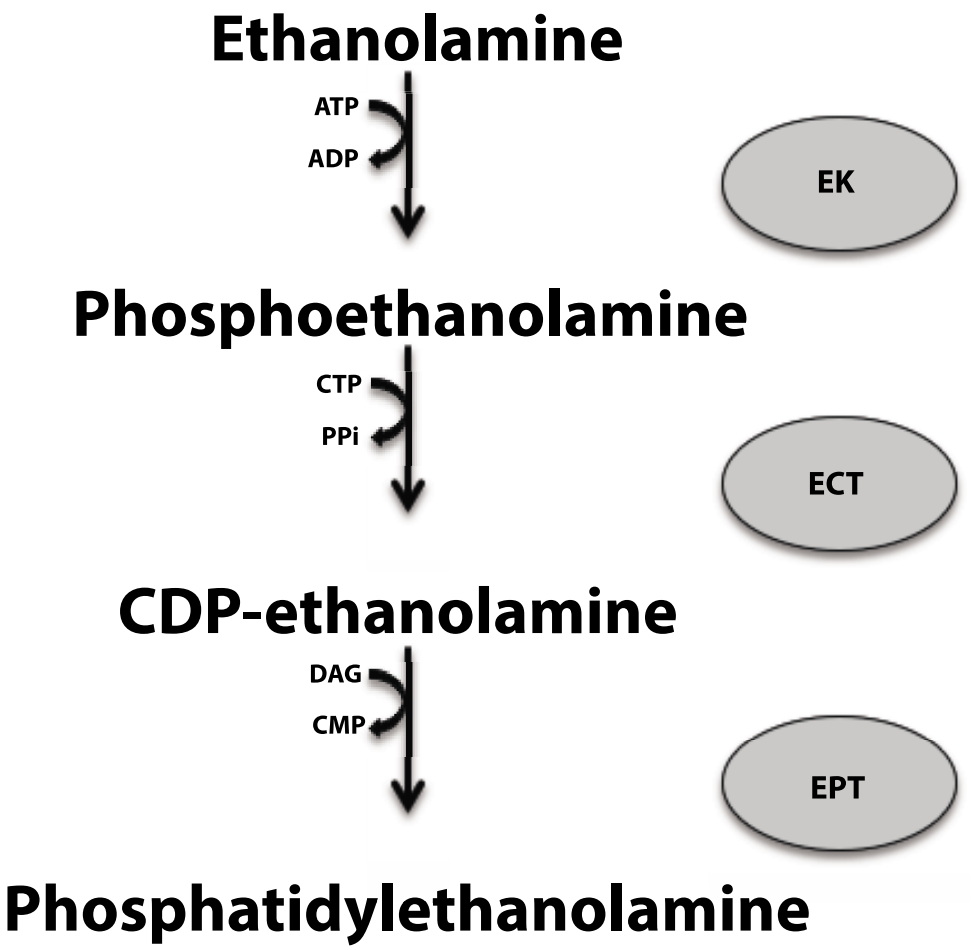

Figure 1.6: **The CDP-ethanolamine pathway in humans.** Ethanolamine gets converted to phosphoethanolamine while adenosine triphosphate (ATP) gets converted to adenosine diphosphate (ADP) by ethanolamine kinase (EK). Phosphoethanolamine gets converted to CDP-ethanolamine by CTP:phosphoethanolamine cytidylyltransferase (ECT) with the addition of cytidine triphosphate (CTP) that gets changed to pyrophosphate (PPi). Lastly, CDP-ethanolamine gets converted to phosphatidylethanolamine by ethanolaminephosphotransferase (EPT) with the addition of diacylglycerol (DAG) and the release of monophosphate (CMP).

gene, *PCYT2*. ECT is concentrated to rough ER-rich areas of the cell which suggests that it also interacts with membranes and a considerable portion of ECT was found to be localized in the cytoplasmic matrix between the RER cisternae which also suggests that ECT may be regulated by membrane binding[64]. Regulation of PE synthesis has been reported at multiple sites in the CDP-ethanolamine pathway with some reports showing evidence that ECT may be one of the rate-limiting enzymes[65]. A global knockout of *Pcyt2* in mice caused embryonic death before day 8.5, but a mouse that was heterozygous for *Pcyt2* was able to survive and maintain lipid homeostasis[66]. In humans, biallelic point mutations in *PCYT2* have been reported to cause a complex hereditary spastic paraplegia[67].

The last step in the CDP-ethanolamine pathway involves the conversion of CDP-ethanolamine and DAG to PE and CMP catalyzed by ethanolaminephosphotransferase (EPT). Two genes code for the EPT proteins in humans, *EPT1* and *CEPT1*. EPT1 utilizes CDP-ethanolamine exclusively, while CEPT1 can utilize both CDP-ethanolamine and CDP-choline as substrates. The precise site of localization for EPT has yet to be determined, but some studies have shown that the Golgi may be involved and that the active site may face the cytoplasm[68]. Multiple mutations in human *EPT1* have been associated with complex hereditary spastic paraplegia [69, 70].

1.6 Phospholipid Synthesis in *Saccharomyces cerevisiae*

Yeast have a similar phospholipid composition to human cells and many of the pathways used for phospholipid synthesis are similar (Figure 1.7). Yeast possess both the CDP-choline pathway and the PE methylation pathway for PC synthesis, and the CDP-

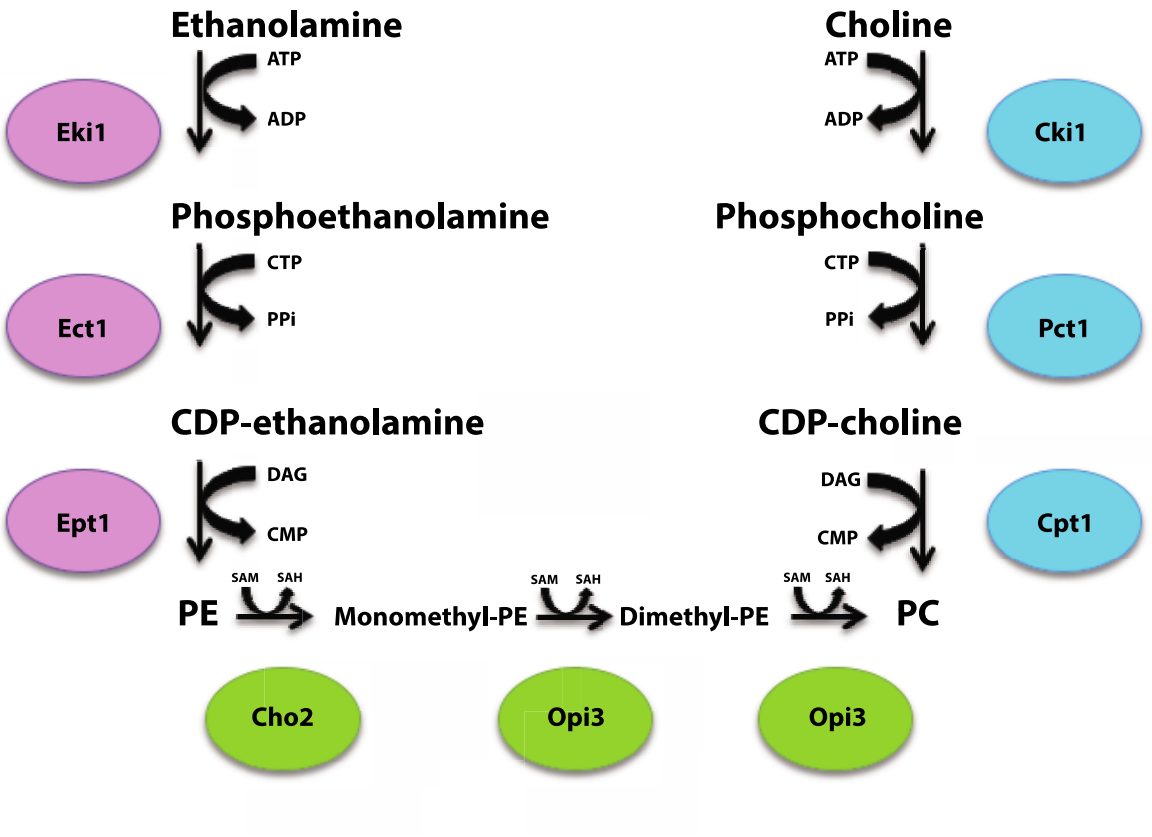

Figure 1.7: **Pathways for PC and PE synthesis in yeast.** Included are the CDP-ethanolamine pathway on the left, the CDP-choline pathway on the right, and the PE methylation pathway on the bottom. The yeast proteins that catalyze each step are indicated in the coloured circles.

ethanolamine pathway for PE synthesis. The steps remain the same in each of the pathways, and the proteins have similar domain structures. Previous work has determined that expression of human open reading frames (ORFs) in yeast can complement the function of many yeast phospholipid-synthesizing enzymes. For this reason, yeast cells have been used to determine the structure and function of human phospholipid synthesizing enzymes expressed in yeast cells where the endogenous enzymes have been genetically inactivated. We used this strategy to address how patient-derived mutations in human *PCYT1A* and *EPT1* affect protein function.

1.7 Inherited Human Diseases Associated with Mutations in the CDP-Choline and CDP-Ethanolamine Pathways

Mutations in several genes within the Kennedy pathways for PC and PE synthesis have demonstrated an association with inherited diseases. Here, I focus on the mutations in *PCYT1A* and *EPT1*, the subjects of this thesis research.

1.7.1 Spondylometaphyseal Dysplasia with Cone-rod Dystrophy

Spondylometaphyseal dysplasia with cone-rod dystrophy (SMD-CRD) is an autosomal-recessive disease that is characterized by severely short stature, progressive bowing of the lower limbs, flattened vertebral bodies (platyspondyly), metaphyseal abnormalities, and visual impairment caused by cone and rod dystrophy[71]. There are ten SMD disorders, but only two of those disorders affect vision with one of those being SMD-CRD. SMD-CRD is caused by biallelic variants in *PCYT1A,* with some patients possessing homozygous mutations and some patients possessing heterozygous variants.

The identified mutations in *PCYT1A* that have been linked to this disease consist of single amino acid changes (A99T, A99V, S114T, E129K, P150A, F191L, R223S, Y240H), a nonsense mutation (R283*), and a frameshift mutation (S323Rfs.38)[42]. The mutations that I chose to use for my studies were A99T, A99V, E129K, P150A, F191L, R223S, and R283*.

1.7.2 Leber Congenital Amaurosis

Inherited retinal dystrophies are a group of conditions that are the most abundant cause of visual impairment that is related to genetics in western society[46]. Leber congenital amaurosis (LCA) is one of these inherited retinal dystrophies. LCA is one of the most severe retinal dystrophies causing severe visual impairment or blindness before the age of 1[72]. LCA is characterized by nystagmus, poor pupillary light response, and retinal function (as detected by electroretinography) is undetectable or severely abnormal[73]. To date, mutations in more than 20 genes have been found to be associated with LCA, but these do not account for all cases of the disease. *PCYT1A* is one of the genes that has associated mutations that have been linked to the manifestation of LCA. There is an autosomal recessive inheritance pattern and the mutations are heterozygous biallelic. The identified mutations in *PCYT1A* that are associated with LCA consist of a single amino acid change (A93T), a nonsense mutation (R283*), and a splice site mutation (L299*17)[42]. For my studies, I chose to work with the A93T and R283* mutations.

1.7.3 Congenital Lipodystrophy with Severe Fatty Liver Disease

Congenital lipodystrophy with severe fatty liver disease (CL-FLD) is the third rare disease that has been associated with mutations in *PCYT1A*. This is also an autosomal recessive disease with heterozygous biallelic mutations. This disease is characterized by the childhood presentation of lipodystrophy (abnormal distribution of fat), severe non-alcoholic fatty liver disease, type II diabetes, dyslipidemia (mainly very low high-density lipoprotein cholesterol levels), and modestly short stature[47]. The *PCYT1A* mutations that have been linked to CL-FLD consist of a single amino acid deletion (E280del), a single amino acid change (V142M), and a frameshift mutation (S333Lfs.164)[42]. The mutant variants that I chose to use for my studies are the V142M and E280del mutations.

1.7.4 Complex Hereditary Spastic Paraplegia

Complex hereditary spastic paraplegias (HSP) are a group of neurodegenerative disorders characterized by spasticity and other neurological (seizures, dementia, ataxia, etc.) or non-neurological (orthopaedic abnormalities, bladder hyperactivity, etc.) features[74]. Similarly to LCA, many genes have been implicated in the manifestation of HSP. *EPT1* is one of the genes that has mutations associated with occurrence of the disease. Mutations that have been identified in *EPT1* that are associated with complex HSPs are autosomal recessive homozygous mutations present on each allele. A mutation in human *EPT1* (R112P) has been previously studied using metabolic radiolabelling of the CDP-ethanolamine pathway in yeast. This study found that the amount of labelled ethanolamine that was incorporated into PE was drastically reduced (3% of that of wild

type) and it was concluded that the R112P mutation in EPT1 caused a decrease in enzyme activity consistent with a loss-of-function mutation[70]. A novel patient-derived mutation in *EPT1* has recently been identified (P45L) and I sought to determine the effect that this mutation has on enzyme activity using metabolic radiolabelling of the CDP-ethanolamine pathway in yeast.

1.8 Objectives

The work that is presented in this thesis is the beginning of a project focussed on discovering how different mutations across the same gene can cause three different inherited diseases. I also looked generally at how mutations in the Kennedy pathway can cause different inherited human diseases. My work focussed specifically on:

i) Determining if human PCYT1A could replace yeast Pct1 function

ii) Generating 10 disease-causing mutant variants identified in human *PCYT1A* and transforming the resulting plasmids into a yeast strain that required functioning PCYT1A for survival

iii) Comparing the disease-associated mutant variants to wild type human *PCYT1A* for differences in growth phenotypes when exposed to various cell stressors

iv) Measuring the biosynthesis of PE when human *EPT1* and a patient-derived *EPT1* mutant were expressed in a yeast strain devoid of the endogenous yeast *EPT1* gene

For this work, we used *in vitro* and *in vivo* assays using *Saccharomyces cerevisiae* as a model organism. Fluorescence microscopy techniques were used to study the localization of human *PCYT1A* in yeast cells. Site-directed mutagenesis and restriction enzyme digestion were used to generate the mutant variants and subclone the mutation-containing DNA fragment into a yeast expression vector. Random sporulation was used to force the yeast cells to undergo meiosis and generate haploid cells. Serial dilution assays were used to study growth phenotypes. Lastly, metabolic radiolabelling was used to study the effect of the patient-derived P45L mutation in human *EPT1* on the synthesis of PE.

CHAPTER 2: MATERIALS AND METHODS

The nomenclature used in this thesis for genes and proteins is as follows: human and yeast genes are written in uppercase and italic font, mice genes are written in italics with the first letter of the gene capitalised, the Delta symbol (Δ) signifies the deletion of a gene, human proteins are written using all capital letters and not in italics, and yeast proteins are written with the first letter capitalised and not italicised.

2.1 Materials

All molecular biology reagents were purchased from New England Biolabs (NEB), Qiagen, or Invitrogen. Custom oligonucleotides were purchased from Integrated DNA Technologies (IDT). Materials used for yeast media were purchased from Sunrise Science Products, VWR Chemicals BDH, Sigma-Aldrich, Fisher Scientific, or Formedium. Radiolabelled [^{14}C]ethanolamine standards were purchased from American Radiolabeled Chemicals.

2.1.1 Plasmids and Primers

Plasmids that had been previously constructed and were used for this study are listed in Table 2.1. Plasmids that I constructed for this project are listed in Table 2.2

2.1.2 Yeast Strains

Yeast strains that were used for this project are listed in Table 2.3.

Table 2.1 **Plasmids Used in this Study**

Plasmid	**Description**
229	TOPO 5' fragment of *PCYT1A* (generated by the McMaster lab)
235	P416 GPD-EPT1 tagged with DDK (generated by the McMaster lab)
p416 GPD	Yeast expression vector used to express human *PCYT1A* in yeast
p416 *PCT1*	*PCT1* present in the p416 backbone and used to express *PCYT1A* under the *PCT1* promoter (generated by the McMaster lab)
PCT1-GFP	*PCT1* with GFP tag in p416 PCT1 backbone (generated by the McMaster lab)
pPM499	P45L point mutation in human *EPT1* in 235 (generated by Maren Brodovsky)
pTR1	Wild-type *PCYT1A* with GPD promoter and mCherry in p416 GPD backbone (generated by the McMaster Lab)
Topo mCherry	mCherry generated by PCR/TOPO-TA cloning in TOPO vector (generated by the McMaster Lab)

Table 2.2 **Plasmids Constructed for this Study**

Plasmid	**ORF/Gene**	**Primers Used/Construction**	**Restriction Sites Used**	**Backbone**
pTR2 (*PCYT1A* R283* with GPD promoter and mCherry)	*PCYT1A*	5'GAAGTGGCAGGAGAA GTCCTGAGAATTCATTG GAAGTTTTCTG 5'CAGAAAACTTCCAATG AATTCTCAGGACTTCTCC TCCCACTTC	*Xba*I/*Eco*RI	p416 GPD
pTR3 (*PCYT1A* E280del with GPD promoter and mCherry)	*PCYT1A*	5'CTTCCAATGAATTCTC GGGACTTCTCCCACTTCT GAATGAGGTCAATGC 5'GCATTGACCTCATTCA GAAGTGGGAGAAGTCCC GAGAATTCATTGGAAG	*Eco*RI/*Sal*I	p416 GPD
pTR4 (*PCYT1A* p.A99V with GPD promoter and mCherry)	*PCYT1A*	5'CGTATTAGGGAAAAGG TTCTTCACTTGCATCAGA GCTCGGGCGTG 5'CACGCCCGAGCTCTGA TGCAAGTGAAGAACCTT TTCCCTAATACG	*Eco*RI/*Sal*I	p416 GPD
pTR5 (wild-type *PCYT1A* with *PCT1* promoter and mCherry)	*PCYT1A*	Subcloned wild-type *PCYT1A* portion of pTR1 into P416 *PCT1* using *Xba*I and *Sal*I restriction enzyme sites	*Xba*I/*Sal*I	p416 *PCT1*
pTR6 (*PCYT1A* R283* with *PCT1* promoter and mCherry)	*PCYT1A*	Subcloned *PCYT1A* R283* (from pTR2) into p416 *PCT1* using *Xba*I and *Sal*I restriction enzyme sites	*XbaI*/*SalI*	p416 *PCT1*
pTR7 (*PCYT1A* E280del with *PCT1* promoter and mCherry)	*PCYT1A*	Subcloned *PCYT1A* E280del (from pTR3) into p416 *PCT1* using *Xba*I and *Sal*I restriction enzyme sites	*Xba*I/*Sal*I	p416 *PCT1*
pTR8 (*PCYT1A* p.A99V with *PCT1* promoter and mCherry)	*PCYT1A*	Subcloned *PCYT1A* p.A99V (from pTR4) into p416 *PCT1* using *Xba*I and *Sal*I restriction enzyme sites	*Xba*I/*Sal*I	p416 *PCT1*

Table 2.2 *Continued from previous page*

Plasmid	**ORF/Gene**	**Primers Used/Construction**	**Restriction Sites Used**	**Backbone**
pTR9 (*PCYT1A* p.E129K with *PCT1* promoter and mCherry)	*PCYT1A*	5'CTTCACGGTGATGAACAAGAATGAGCGCTATGACG 5'CGTCATAGCGCTCATTCTTGTTCATCACCGTGAAG	*Xba*I/*Eco*RI-HF	p416 *PCT1*
pTR10 (*PCYT1A* p.A93T with *PCT1* promoter and mCherry)	*PCYT1A*	5'CTTATTTCACTCTGGTCACACCCGAGCTCTGATGCAAG 5'CTTGCATCAGAGCTCGGGTGTGACCAGAGTGAAATAAG	*Xba*I/*Eco*RI-HF	p416 *PCT1*
pTR11 (*PCYT1A* p.A99T with *PCT1* promoter and mCherry)	*PCYT1A*	5'GCTCTGATGCAAACGAAGAACCTTTTCCCTAATACG 5'CGTATTAGGGAAAAGGTTCTTCGTTTGCATCAGAGC	*Xba*I/*Eco*RI-HF	p416 *PCT1*
pTR12 (*PCYT1A* p.F191L with *PCT1* promoter and mCherry)	*PCYT1A*	5'GAGGCAGGCATGCTTGCTCCAACACAG 5'CTGTGTTGGAGCAAGCATGCCTGCCTC	*Xba*I/*Eco*RI-HF	p416 *PCT1*
pTR13 (*PCYT1A* p.R223S with *PCT1* promoter and mCherry)	*PCYT1A*	5'GGAACCTGCAGAGCGGCTACACAGCAAAGG 5'CCTTTGCTGTGTAGCCGCTCTGCAGGTTCC	*Xba*I/*Eco*RI-HF	p416 *PCT1*
pTR14 (*PCYT1A* p.V142M with *PCT1* promoter and mCherry)	*PCYT1A*	5'GCACTGCCGCTACATGGATGAGGTGGTGAG 5'CTCACCACCTCATCCATGTAGCGGCAGTGC	*Xba*I/*Eco*RI-HF	p416 *PCT1*
pTR15 (*PCYT1A* p.P150A with *PCT1* promoter and mCherry)	*PCYT1A*	5'GTGAGGAATGCGGCCTGGACGCTGAC 5'GTCAGCGTCCAGGCCGCATTCCTCAC	*Xba*I/*Eco*RI-HF	p416 *PCT1*

Table 2.3 **Yeast Strains Used in this Study**

Yeast Strain	Genotype/Description
106	BY4741 *cho2Δ::KAN*
1097	BY4742 *cho2Δ::KAN opi3Δ::LEU2*
1098	519 mated with 1097 (diploid strain)
245	BY4741 *pct1Δ::KAN*
519	BY4741 *pct1Δ::HYG*
520	BY4742 *pct1Δ::HYG*
BY4741	**a** *his3Δ1 leu2Δ0 met15Δ0 ura3Δ0*
BY4742	**α** *his3Δ1 leu2Δ0 lys2Δ0 ura3Δ0*
HJ001	**a** *his3Δ1 leu2Δ3 leu2Δ112 ura3Δ52 trp1Δ289 cpt1::LEU2*
HJ091	**a** *his3Δ1 leu2Δ3 leu2Δ112 ura3Δ52 trp1Δ289 cpt1::LEU2 ept1-1*
yTR1	520 mated with 106 transformed with pTR1
yTR2	520 mated with 106 transformed with pTR2
yTR3	520 mated with 106 transformed with pTR3
yTR4	520 mated with 106 transformed with pTR4
yTR5	1098 strain transformed with pTR5
yTR6	1098 strain transformed with pTR6
yTR7	1098 strain transformed with pTR7
yTR8	1098 strain transformed with pTR8
yTR9	1098 strain transformed with pTR9
yTR10	1098 strain transformed with pTR10
yTR11	1098 strain transformed with pTR11
yTR12	1098 strain transformed with pTR12
yTR13	1098 strain transformed with pTR13
yTR14	1098 strain transformed with pTR14
yTR15	1098 strain transformed with pTR15

2.1.3 Antibodies

Antibodies that were used in the western blots performed for this project were purchased from Abcam and Origene and are listed in Table 2.4.

2.1.4 Restriction Enzymes

All restriction enzymes that were used in this project were purchased from New England Biolabs and are listed in Table 2.5.

2.2 Protocols for Bacteria and Recombinant DNA Techniques

2.2.1 PCR and *TOPO-TA Cloning*

The TOPO-TA cloning kit that was used was purchased from Invitrogen. In order to do the TOPO-TA cloning, PCR was performed to amplify the required DNA fragment. To do so, the reaction was set up in a 0.2 mL PCR tube for 50 µL total reaction volume as follows: 5 µL of 10X High Fidelity PCR Buffer, 2 µL of 50 mM $MgSO_4$, 1 µL of 10 mM dNTP Mix, 1 µL of 10 µM forward primer, 1 µL of 10 µM reverse primer, less than 500 ng of template DNA, 0.2 µL of Platinum *Taq* DNA Polymerase High Fidelity, and distilled water up to 50 µL. The reaction was mixed by pipetting up and down and the PCR tube was spun briefly in a centrifuge to bring all of the contents of the tube to the bottom. The tube was then placed in a thermal cycler with the following cycles: the initial denaturation was held at 94°C for 30 seconds to 2 minutes, 25-35 PCR cycles with denaturing (94°C for 15 seconds), annealing (~55°C (depending on primer T_m) for 30 seconds, and extension (68°C for 1 minute/kb) steps, a final extension at 68°C for 7

Table 2.4 **Antibodies Used in this Study**

Antibody	**Concentration Used**	**Source**
Rabbit monoclonal to mCherry (ab213511)	1:2000	Abcam
Anti-DDK (FLAG) monoclonal antibody (mouse)	1:2000	Origene

Table 2.5 **Restriction Enzymes Used in this Study**

Restriction Enzyme	**Cut Site**
*Eco*RI	5'…G|AATTC…3' 3'…CTTAA|G…5'
*Eco*RI-HF	5'…G|AATTC…3' 3'…CTTAA|G…5'
*Mlu*I	5'…A|CGCGT…3' 3'…TGCGC|A…5'
*Nhe*I	5'…G|CTAGC…3' 3'…CGATC|G…5'
*Sac*I	5'…GAGCT|C…3' 3'…C|TCGAG…5'
*Sal*I	5'…G|TCGAC…3' 3'…CAGCT|G…5'
*Sal*I-HF	5'…G|TCGAC…3' 3'…CAGCT|G…5'
*Sna*BI	5'…TAC|GTA…3' 3'…ATG|CAT…5'
*Xba*I	5'…T|CTAGA…3' 3'…AGATC|T…5'

minutes, and then a hold at 4°C. The PCR products had their identity verified using agarose gel electrophoresis. Then the fresh PCR product was used for TOPO-TA cloning. To set up this reaction, 0.5-4 µL of the product was mixed with 1 µL of the salt solution, 1 µL of the TOPO vector, and water up to a final volume of 6 µL. The reaction was mixed by pipetting up and down and the PCR tube was centrifuged briefly to bring all contents to the bottom. The solution was left to incubate for 5 minutes at room temperature. Then the reaction was used to transform TOP10 Chemically Competent Cells.

2.2.2 Site-directed Mutagenesis

All site-directed mutagenesis was completed using the QuikChange II kit from Agilent. Reactions were prepared in 0.2 mL PCR tubes. The reaction consisted of 5 µL of 10x reaction buffer, 125 ng of oligonucleotide primer #1, 125 ng of oligonucleotide primer #2, 1 µL of dNTP mix, 5-50 ng of dsDNA template, and water up to 50 µL. Then 1 µL of *PfuUltra* HF DNA polymerase was added to the tube. The reaction was mixed by pipetting up and down and then the tube was centrifuged briefly to bring the contents to the bottom. The thermocycler was then programmed with the following parameters: 1 cycle at 95°C for 30 seconds, then 16 cycles of 95°C for 30 seconds, 55°C for 1 minute, and 68°C for 1 minute per kb of plasmid length. Following the temperature cycling, the tube was placed on ice to cool the reaction. Then 1 µL of the *Dpn*I restriction enzyme was added to the tube to degrade the template DNA. The reaction was mixed by pipetting up and down and the contents of the tube were brought to the bottom by briefly centrifuging. This reaction was incubated at 37°C for 1 hour to allow complete digestion

of the template DNA. Following this, XL10-Gold Ultracompetent Cells were transformed with the site-directed mutagenesis product, plated on LB+Ampicillin, and put to grow at 37°C overnight. Bacterial colonies were then grown in liquid culture and verified by restriction enzyme digestion and DNA sequencing.

2.2.3 Restriction Enzyme Digestion

Plasmid DNA was digested using restriction enzymes from New England Biolabs (Table 2.4). For a 20 µL reaction 0.6-0.8 µg of plasmid DNA (up to 5 µL), 2 µL of the appropriate buffer, 1 µL of the first restriction enzyme, 1 µL of the second restriction enzyme, and water up to 20 µL were added to a 1.5-mL microcentrifuge tube. The tubes were briefly centrifuged to bring contents to the bottom and the reaction was mixed by pipetting up and down. The tubes were placed in a 37°C incubator for approximately 3 hours. Following this, 0.5 µL of calf intestinal alkaline phosphatase was added to the tube containing the vector and this was incubated at 37°C for an additional 10 minutes. A 1.5% agarose gel was made containing ethidium bromide. The samples were loaded into the lanes in the agarose. The gel was placed in an electrophoresis tank and was run at 80 V for approximately 45 minutes.

2.2.4 Purification of DNA from Agarose Gel Using the GeneClean II Kit

DNA was viewed in the agarose gel containing ethidium bromide using UV light and a razor blade was used to excise the appropriate DNA bands based on their molecular weight. The gel was placed into a 1.5-mL microcentrifuge tube and the weight of the piece of gel was determined and converted to approximate volume (100 µg = 100 µL).

Since TAE gels were used, 3 volumes of the NaI solution were added to the microcentrifuge tube. The tube was incubated at 55°C in a heating block until the gel was melted (approximately 5 minutes). The tube was vortexed periodically during the melting process. Following melting, GLASSMILK was added to the based on 1 µL of GLASSMILK binding to 1-2 µg of DNA. The solution was mixed and then incubated at room temperature for 15 minutes on a spinning wheel. The sample was pelleted using a tabletop centrifuge at maximum speed for 1 minute. The supernatant was removed and the pellet was resuspended with 500 µL of NEW Wash and the sample was centrifuged for 5 seconds. The supernatant was discarded and the pellet was rewashed with the NEW Wash. The tube was then placed in the heating block at 55°C for approximately 15 minutes with the lid open to dry the pellet. A volume of water was added to the pellet that was equal to the amount of GLASSMILK that was added. The pellet was resuspended and left to sit at room temperature for 5 minutes. The tube was centrifuged for 30 seconds on maximum speed and the DNA-containing supernatant was removed and saved.

2.2.5 Ligation Protocol with T4 DNA Ligase

Using a 1.5-mL microcentrifuge tube, the following reaction was set up on ice: T4 DNA ligase buffer (10X) (2 µL), vector DNA (0.020 pmol), insert DNA (0.060 pmol), nuclease-free water (to 20 µL total), T4 DNA ligase (1 µL). The sample was mixed by pipetting up and down and then a tabletop microcentrifuge was used for 5 seconds to bring the contents to the bottom of the tube. For cohesive (sticky) ends, the sample was incubated at room temperature for 10 minutes. The reaction was then heat inactivated by

using a heating block set at 65°C for 10 minutes. The tube was chilled on ice and 1-5 µL of the reaction was transformed into competent bacterial cells.

2.2.6 Bacterial Transformation

Bacterial transformation was performed by thawing an aliquot of chemically competent *Escherichia coli* (TOP10) on ice and adding approximately 100 ng of plasmid DNA. The mix was incubated on ice for 30 minutes and then cells were heat shocked using a 42°C water bath for 30 seconds. The tube was placed on ice for 2 minutes and 250 µL of S.O.C. medium was added. The cells were placed in a 37°C incubator with shaking for 1 hour to allow recovery. Following this, 250 µL of the transformed cell mix was plated on selective agar plates (LB + ampicillin).

2.2.7 Isolation of DNA from transformed Escherichia coli Using the QIAPrep Spin Miniprep Kit

Bacterial cultures up to 5 mL were grown overnight in LB + ampicillin medium. Samples were pelleted by centrifugation at 3000 rpm for 10 minutes. The supernatant was discarded and the pellet was resuspended in 250 µL of Buffer P1 and transferred to a 1.5-mL microcentrifuge tube. Next, 250 µL of Buffer P2 was added and the tube was mixed thoroughly by inversion. This lysis reaction was not allowed to proceed for more than 5 minutes. To stop it, 350 µL of Buffer N3 was added to the tube and the sample was mixed by inversion. To pellet the contents, the tube was centrifuged at 13000 rpm for 10 minutes. The supernatant (800 µL) was transferred to a QIAPrep spin column and the column was centrifuged at maximum speed for 1 minute. The flow-through was

discarded and 0.5 mL of Buffer PB was added to the column. The column was centrifuged at maximum speed in a microfuge for 1 minute and the flow through was discarded. The column was washed twice by adding 750 µL of Buffer PE, centrifuging for 1 minute at maximum speed, and discarding the flow-through. Following the wash, the column was centrifuged for an additional minute to discard any extra flow-through. The column was placed in a 1.5-mL microcentrifuge tube and 50 µL of water was added to the centre of the column. This was allowed to rest on the bench for 2 minutes before centrifuging and removing the column.

2.3 Microscopy

2.3.1 Fluorescence Microscopy

Microscopy was done using a Zeiss axiovert microscope. To visualize the GFP and m-cherry proteins, yeast cells were grown to mid-log phase at 30°C and a 500 µL aliquot was pipetted into a 1.5-mL Eppendorf tube. The cells were pelleted using a tabletop centrifuge at 3000 rpm for 3 minutes. The supernatant was removed and the pellet was resuspended in 50 µL of water. A 4 µL aliquot was pipetted onto a glass slide. A coverslip was placed on top of it and sealed with clear nail polish. The cells were imaged using a 100x objective with oil and localization assays were completed with cells expressing mCherry-tagged proteins or GFP-tagged proteins. The excitation and emission wavelengths used for mCherry were 587 nm and 610 nm. The excitation and emission wavelengths used for GFP were 488 nm and 510 nm. The images were processed using the AxioVision program.

2.3.2 CCTα Localization Assay

Liquid cultures were started in 2 mL of SC-uracil medium and grown overnight at 30°C with shaking. The next morning, the OD_{600} of the culture was read using 1 mL of the undiluted sample and a spectrophotometer. The cultures were diluted to 5 mL and were grown in a 30°C shaker for 4 hours. Following this growth period, samples were split into two tubes and 1 mL of media containing 2 mM choline was added to one tube while choline-free media was added to the other. Samples were grown for 2 more hours at 30°C and analyzed using fluorescence microscopy.

2.4 Yeast Protocols

2.4.1 Yeast Transformation

Yeast cells were transformed with plasmid DNA using a slightly modified version of the lithium acetate/polyethylene glycol method[75]. Cells were grown overnight in 5 mL of YPD media at 30°C. The following morning, cells were diluted to 50 mL with YPD and put back in the 30°C incubator to grow for 3-4 hours. While the cells were growing, two solutions were made. The lithium acetate solution was made of 1:1:8 1 M lithium acetate/10X TE (pH 8)/H_2O. The TE/LiAc/PEG solution was made of 1:1:8 1 M lithium acetate/10X TE (pH 8)/50% polyethylene glycol. Following the growth period, cells were pelleted using centrifugation at 2500 rpm for 5 minutes. The supernatant was removed and the cells were washed with 25 mL of water and pelleted by centrifugation at 2500 rpm for 5 minutes. The supernatant was removed and cells were resuspended in 1 mL of lithium acetate mix. The cells were transferred to 1.5-mL Eppendorf tubes and pelleted using a tabletop microcentrifuge at max rpm for 1 minute. Supernatant was removed and

cells were resuspended in 50 µL of lithium acetate solution per transformation. Round bottom tubes were set for each separate transformation. For each transformation, 2 µL of plasmid (0.4-0.8 µg/µL), 10 µL of sheared herring sperm DNA, 50 µL of the resuspended cells in TE/LiAc, and 350 µL of the TE/LiAc/PEG solution were pipetted into the tubes. The samples were mixed by vortexing and then incubated in a 30°C shaker for 1.5 hours. Cells were then heat shocked using a 42°C water bath for 10 minutes. Following this, 3 mL of water was added to each tube and they were mixed by vortexing. Cells were pelleted by centrifugation at 2500 rpm for 5 minutes and supernatant was removed. The pellet was resuspended in 200 µL of water and the cells were plated on selective media. The plates were put in a 30°C incubator to grow for 2-3 days.

2.4.2 Random Sporulation

The yeast strains 1097 and 519 were manually mated. The resulting colonies were comprised of diploid cells. These diploid colonies were transformed with plasmids pTR5 through pTR15. The transformed diploid cells were suspended in 2 mL of SC-uracil medium and grown at 30°C for 1 day. Cells were centrifuged (2500 rpm for 5 minutes) and the supernatant was removed. The cells were washed with 2 mL of sterile water, centrifuged at 2500 rpm for 5 minutes, and the supernatant was removed. The cells were resuspended in 2 mL of PSP2 media supplemented with histidine (1%), methionine (1%), lysine (1.5%), and choline (1 mM) and put in a shaker at 30°C to grow overnight. The PSP2 media was comprised of 1 g potassium acetate, 0.17 g of yeast nutritional broth (without ammonium sulphate), 0.5 g ammonium sulphate, 0.1 g yeast extract, and 100 mL of water. The next day, cells were washed twice with 2 mL of sterile water and

pelleted by centrifugation at 2500 rpm for 5 minutes. The pellet was resuspended in 2 mL of 1% KAc supplemented with histidine (1%), methionine (1%), lysine (1.5%), and choline (1 mM). The cells were put on a rotating wheel to grow at room temperature for 3-6 days. Samples were ready for hydrophobic spore isolation when multiple asci could be seen while looking at the sample using brightfield microscopy. Cells were centrifuged at 2500 rpm for 5 minutes and the supernatant was removed. The pellet was resuspended in 1 mL of 100 µg/mL Zymolyase 10,000 and incubated at 30°C for 25 minutes. A 500 µL aliquot was pipetted into a 1.5-mL Eppendorf tube and centrifuged at 14000 g for 30 seconds using a tabletop microcentrifuge. The supernatant was discarded and cells were resuspended in 1 mL of water, centrifuged, and then resuspended in 100 µL of water. Each tube was then agitated in an upright position by vortexing on maximum speed for 2 minutes. The liquid in the tube was removed and the walls of the tube were rinsed several times with water. The spores were resuspended by adding 0.01% Nonidet-P40 and sonicating for 3 minutes. The spore preparation was diluted and approximately 200 spores were plated on solid medium. For our work, the medium used was SC-uracil-leucine supplemented with choline, G418, and hygromycin.

2.4.3 Haploid Cell Selection

Following random sporulation, verification of haploid cell isolation was required. This was done by replica plating on selective media. Single colonies from the random sporulation plates were streaked out onto SC-uracil-leucine+KAN+HYG+choline plates. These were placed into a 30°C incubator to grow for 2 days. Following the 2-day growth period, the plates were inverted and pressed onto a piece of felt. The cells that transferred

could be used to replica plate onto different media. For this experiment, the replica plating was done onto plates that were lacking lysine and plates that were lacking methionine. One of the strains that we used to make the diploid was a lysine prototroph and the other strain was a methionine prototroph. This means that a haploid cell could be identified by a lack of growth on –lys plates, -met plates, or both. Another test involving yeast mating types was used to verify that the colony that was isolated was indeed a single colony. Suspected haploid cells were streaked onto two separate YPD plates. Cells on one plate were manually mated with a mating type **α** strain and cells on the other plate were mixed with a mating type **a** strain. The plates were placed in a 30°C incubator to grow for 2 days. Following the growth period, the cells were replica plated onto SM media and placed in an incubator at 30°C to grow for 2 days. Cells that grew on one plate but not the other were assumed to be from single isolated colonies.

2.4.4 Serial Dilution Growth Assay

Cells were grown overnight in SC-uracil+choline medium to stationary phase at 30°C in an incubator with shaking. The next morning, the cells were pelleted by centrifugation (2500 rpm for 5 minutes) and the samples were washed with sterile water at least twice. The pellet was resuspended using 2 mL of SC-uracil medium. The OD_{600} of the samples were read and the cell density of each sample was normalized to an OD_{600} of 0.8. Samples were serially diluted (1:10) using a 96-well cell culture plate with a final volume of 200 µL in each well. Cells were spotted onto various solid media using a replica pinner. The plates were placed in a 30°C incubator (unless studying growth at a different temperature) to grow for 3-12 days. Plates were checked each day after pinning

to ensure that no growth phenotypes were missed. Each plate was imaged using a Bio-Rad VersaDoc.

2.5 Techniques for Lipid Analysis

2.5.1 Metabolic Labeling of PE and Metabolites of the CDP-ethanolamine Pathway Using [^{14}C]Ethanolamine

2 mL liquid cultures of yeast in SC-uracil media were grown to mid-log phase at 30°C. The OD_{600} of the cultures was determined and all samples were normalized to the least concentrated sample to guarantee a similar number of cells in each tube. Following this, cells were pelleted by centrifugation at 2500 rpm for 5 minutes using a microcentrifuge. The supernatant was removed and the samples were washed with 2 mL of ammonium sulphate-free SC-uracil medium and centrifuged again at 2500 rpm for 5 minutes. After removing the supernatant, 4 mL of [^{14}C]ethanolamine labeled SC-uracil-ammonium sulphate medium was added to each tube, and samples were incubated at 30°C for 1 hour. Following incubation, 100 µL of 0.5 M NaN_3/NaF was added to each tube and they were put on ice for 3 minutes to kill the cells. The cells were pelleted by centrifugation at 2500 rpm for 5 minutes and the supernatant was removed. Then the cells were washed with 3 mL of cold water and centrifuged at 2500 rpm for 5 minutes. The supernatant was removed and cells were taken up in 1 mL of water and transferred to 1.5 mL bead-beater screw-cap tubes. The samples were centrifuged at 2500 rpm for 5 minutes using a tabletop centrifuge, the supernatant was removed and lipid extraction followed.

2.5.2 Lipid Extraction

Pelleted cells were resuspended in 1 mL of 1:1 chloroform/methanol (v/v) solution. Samples were vortexed to partially resuspend the pellet and the tubes were filled approximately 1/8 of the way up with 0.5 mm acid-washed glass beads. Cells were agitated by bead beating on maximum speed for 1 minute and the liquid was transferred to a glass test tube with a screw-top. The glass beads were washed with 1 mL of 2:1 chloroform/methanol and the wash was combined with the first extract in the glass test tube. A 100 µL sample was taken from this to measure the total uptake of radiolabeled material and was placed in a scintillation counter tube to dry. This was counted using a Beckman LS 6500 scintillation counter. 1 mL of 5:1 chloroform/methanol and 1.5 mL of water was added to the extract. Test tubes were vortexed on a shaker for 5 minutes. These were then centrifuged at 2500 rpm for 10 minutes to phase separate. The resulting solution was composed of three layers. The top layer was the aqueous phase, the middle was a protein layer, and the bottom layer was the organic phase. From the top layer a 100 µL aliquot was taken to measure radiolabelled content in the total aqueous metabolites and a 400 µL aliquot was taken to use for thin-layer chromatography to separate the aqueous metabolites. The middle (protein) layer was discarded. From the bottom layer, a 100 µL aliquot was taken to measure total radiolabel present in the organic (lipid containing) phase, a 400 µL aliquot was taken for thin-layer chromatography to separate the organic metabolites, and a 700 µL aliquot was taken and put into a glass test tube to measure the total lipid phosphorus content.

2.5.3 Lipid Phosphorus Determination

Samples of 700 µL from the organic phase were dried using N_2 gas. Phosphate standards were prepared using a solution of 1 mM potassium dihydrogen phosphate. Concentrations of standards were as follows: 0 nm, 20 nm, 40 nm, 60 nm, 80 nm, and 100 nm phosphate. In each tube, the volume was brought up to 300 µL with water and 150 µL of perchloric acid was added. The samples were incubated overnight at 150°C in a heating block with marbles on top of the tubes. The next morning, 700 µL of water was added to each tube and they were left to rest at room temperature for 20 minutes. This was followed by the addition of 500 µL of 0.9% ammonium molybdate and 150 µL of 10% ascorbic acid. The solution was mixed and incubated at 45°C for 30 minutes. Absorbance was measured at 820 nm using a spectrophotometer.

2.5.4 Thin-Layer Chromatography

Aqueous and organic samples were dried overnight in 1.5-mL Eppendorf tubes using a speed-vac. Aqueous samples were resuspended in 15 µL of 7:3 H_2O/ethanol and were incubated at room temperature for 30 minutes. Organic samples were resuspended in 20 µL of $CHCl_3$ and incubated at room temperature for 30 minutes. Samples were spotted onto silica thin-layer chromatography (TLC) plates and dried. The aqueous phase TLC plates were developed using a solvent comprised of 50:50:5 CH_3OH/0.6% NaCl/NH_4OH (150 mL total). The organic phase TLC plates were developed using a solvent comprised of 70:30:2:2 $CHCl_3$/MeOH/glacial acetic acid/H_2O (150 mL total). The plates were developed until the solvent front reached approximately 1 cm from the top of the plate. The plates were dried and radiolabel for each metabolite was detected

using a TLC radiochromatograph, and compared to known standards, to identify bands corresponding to each CDP-ethanolamine pathway metabolite. The organic phase plate was also stained using iodine vapour. The plate was placed in a chamber filled with the vapour and was left to develop for 10 minutes. When the plate was removed from the tank, phosphatidylethanolamine and phosphatidylcholine were visible. The locations of these were marked on the silica using a pencil. Once the locations of all of the metabolites were known, they were scraped from the plate and the silica for each metabolite from each lane was placed into a scintillation counter vial, scintillation cocktail was added, and radioactivity was determined using a Beckman LS 6500 scintillation counter.

2.6 Using SDS-Page and Western Blotting to Measure Protein Expression

Firstly, a 7.5% acrylamide gel was made by making a running gel and a stacking gel. The running gel was prepared as follows: 0.94 mL of 40% acrylamide/bis-acrylamide, 1.25 mL of 1.5 M Tris-HCl (pH 8.8), 50 µL of 10% SDS, 2.74 mL of water, 2.5 µL of TEMED, and 25 µL of 10% APS. The running gel was pipetted in between gel plates held in a casting tray and left to set for approximately 20 minutes. Any bubbles were removed by adding a small amount of saturated butanol, which was removed using a Kimwipe. The stacking gel was then prepared as follows: 125 µL of 40% acrylamide/bis-acrylamide, 315 µL of 0.5 M Tris-HCl (pH 6.8), 12.5 µL of 10% SDS, 0.795 mL of water, 1.25 µL of TEMED, and 12.5 µL of 10% APS. Once the running gel was set, the stacking gel was loaded on top of it. A comb was inserted and the gel was left to set for another 20 minutes. The gel electrophoresis apparatus was set up and the

centre of the electrophoresis chamber was filled with 1x SDS running buffer. The comb was removed from the gel and the gel was loaded with the protein samples and a ladder. The gel was run at 20 mA for approximately 90 minutes.

For the Western blot, a nitrocellulose membrane that was about the same size as the gel was cut and soaked in 1x transfer buffer for a few minutes before using. The cassette with the membrane, sponges, paper, and gel was assembled and a roller was used to push out any bubbles that may have gotten trapped. The electrophoresis chamber was prepared with an ice pack and a stir bar, and transfer buffer. The electrophoresis was run at 20 V overnight. The next day, the membrane was soaked in Ponceau S for about 5 minutes until the proteins were visible. The membrane was cut down to size using a razor blade. The membrane was then rinsed with water several times to remove the red colour. Next, the membrane was soaked in a 1:1 solution of TBS buffer and odyssey buffer in a small plastic box and placed on a Belly Dancer at level 3 for about 1 hour. The membrane was then placed in a solution of 3:1 TBS-T buffer and odyssey buffer and placed on a Belly Dancer at level 3 for 1 hour. Following this, the membrane was probed with the appropriate antibodies. After probing overnight, the buffer was drained off and the membrane was washed several times with TBS-T. The membrane was visualized using the Odyssey.

CHAPTER 3: RESULTS

The Kennedy pathway is an important pathway for eukaryotic cells as it is responsible for the synthesis of major phospholipids that make up eukaryotic cell membranes[76]. The pathway itself consists of two branches, the CDP-choline branch and the CDP-ethanolamine branch that are responsible for synthesizing PC and PE, respectively. Mutations that occur in any step of either branch of the Kennedy pathway have been associated with inherited human diseases[9, 32-34, 53, 63, 67, 69, 70].

The CDP-choline pathway consists of three steps where the second step, catalyzed by PCYT1A, is the rate-determining step. Mutations that have been reported in *PCYT1A* have been associated with one of three inherited diseases[42]. It is currently unknown how diseases with very different phenotypes appear to be caused by mutations in the same gene. The objective of my studies was to determine how these different mutations in *PCYT1A* affect the function of the enzyme, and if there is a relationship between the effect of the mutation in the enzyme and the disease that is occurring. This was done by determining if each disease-causing *PCYT1A* mutation resulted in a change in the ability of cells to respond to cell stressors.

The CDP-ethanolamine pathway also consists of three steps[76]. A new mutation was identified in the enzyme that catalyzes the third step of the pathway. This mutation has been associated with complex hereditary spastic paraplegia. We sought to determine if this newly identified mutation in *EPT1* affected the biosynthesis of PE by metabolic radiolabelling of the CDP-ethanolamine pathway.

For my studies, I used *Saccharomyces cerevisiae* as a model organism. This species of yeast has been previously used to study some of the human Kennedy pathway

enzymes[51,77,78]. The CDP-choline and CDP-ethanolamine pathways, and the domain structures of each enzyme, are conserved from yeast to humans.

3.1 Human *PCYT1A* Can Replace *PCT1* Function in *Saccharomyces cerevisiae*

One of the main objectives of my study was to determine if *Saccharomyces cerevisiae* could be used as a model organism for the study of disease-causing mutations in human *PCYT1A.* We first sought to determine if human *PCYT1A* is able to replace *PCT1* function in yeast.

To determine if human *PCYT1A* is able to replace *PCT1* function in yeast, we created a plasmid for the expression of human *PCYT1A* in yeast. The human *PCYT1A* open reading frame was subcloned into the low-copy yeast expression vector, p416 GPD. The p416 GPD vector drives gene expression by the constitutive *GPD1* promoter. DNA sequencing confirmed that the *PCYT1A* open reading frame was successfully subcloned into p416 GPD, and that there were no errors in the *PCYT1A* coding sequence.

To determine if human *PCYT1A* could replace the function of *PCT1* in yeast, we sought to create a yeast strain where cell growth was dependent on *PCYT1A* function. Yeast cells contain two pathways for the synthesis of PC, the PE methylation pathway catalyzed by Cho2 and Opi3 as well as the CDP-choline branch of the Kennedy pathway where Pct1 is the rate-determining step. A yeast strain devoid of both pathways is not viable. A diploid strain heterozygous for *cho2*Δ *opi3*Δ *pct1*Δ was created by mating a haploid *cho2*Δ *opi3*Δ strain with a haploid *pct1Δ* strain. The resulting diploid strain was transformed with the plasmid expressing human *PCYT1A*. Diploid cells were forced to undergo sporulation (meiosis) by culturing cells in sporulation (low nutrient) medium.

After sporulation, haploid cells were selected using the nutritional auxotrophies present in each inactivated gene, as well as the plasmid expressing *PCYT1A*, in medium supplemented with 100 μM choline. The choline addition is necessary as PC can only be synthesized by the CDP-choline pathway in haploid *cho2*Δ *opi3*Δ *pct1*Δ cells expressing human *PCYT1A*. To ensure that the cells were indeed haploids, two different procedures were used. We confirmed their genotype using a combination of nutritional auxotrophies that would only be present in a resulting haploid strain, and we also ensured that the cells could mate (as only haploid cells can mate). Using these methods we were able to successfully isolate *cho2*Δ *opi3*Δ *pct1*Δ haploid cells expressing human *PCYT1A*. We chose three different haploids expressing *PCYT1A*. All further experiments were performed using a different strain each time to ensure that a random genetic event did not occur during strain construction that could affect the strain phenotype(s). Further replicates using all three strains in a single experiment will be required to verify that the phenotypes are similar across all strains. As we were able to successfully isolate *cho2*Δ *opi3*Δ *pct1*Δ haploid cells expressing human *PCYT1A*, this indicates that human PCYT1A is able to replace essential *PCT1* functions in yeast.

We sought to further confirm that human *PCYT1A* could replace yeast *PCT1* function. If the PE methylation pathway is inactivated, and if human *PCYT1A* can replace yeast *PCT1* function, then the *cho2*Δ *opi3*Δ *pct1*Δ haploid cells expressing human *PCYT1A* should not be able to grow on medium lacking choline. To test this, we serially diluted cells grown in liquid culture containing choline, and plated the serial dilutions on solid agar plates containing either 200 μM choline or no choline. We observed that yeast cells transformed with human *PCYT1A* were able to grow in the presence of choline, but

showed severely reduced growth in the absence of the nutrient (Figure 3.1). A similar phenotype was observed in cells expressing yeast *PCT1* in the absence of the PE methylation pathway.

We were able to successfully create a yeast strain where the PE methylation pathway was inactivated, and where cell growth was dependent on the Kennedy pathway. In addition to this, we determined that cell growth was similar in a yeast strain where the rate-determining step in the Kennedy pathway was catalyzed by either yeast Pct1 or human PCYT1A.

3.2 *PCYT1A* Translocates to Membranes in *Saccharomyces cerevisiae* in the Absence of Exogenous Choline

Both yeast Pct1 and human PCYT1A proteins are soluble proteins that translocate to cell membranes when membrane synthesis is required[42,79]. Both proteins are found to be nucleoplasmic when inactive and translocate to nuclear or ER membranes when active[37,79]. In yeast, it has been found that Pct1 detaches from the membrane and localizes to the nucleoplasm upon the addition of choline to the growth medium[79]. When the growth medium lacks choline, the enzyme localize to membranes. We sought to determine if human PCYT1A is successfully imported into the nucleus and translocates on and off membranes in a similar manner when expressed in yeast.

A wild type yeast strain was used to express an mCherry tagged version of PCYT1A. The Kennedy pathway is not essential for life in wild type yeast due to the presence of the PE methylation pathway. This enables choline addition experiments to be performed. The *PCYT1A* open reading frame containing the coding sequence for

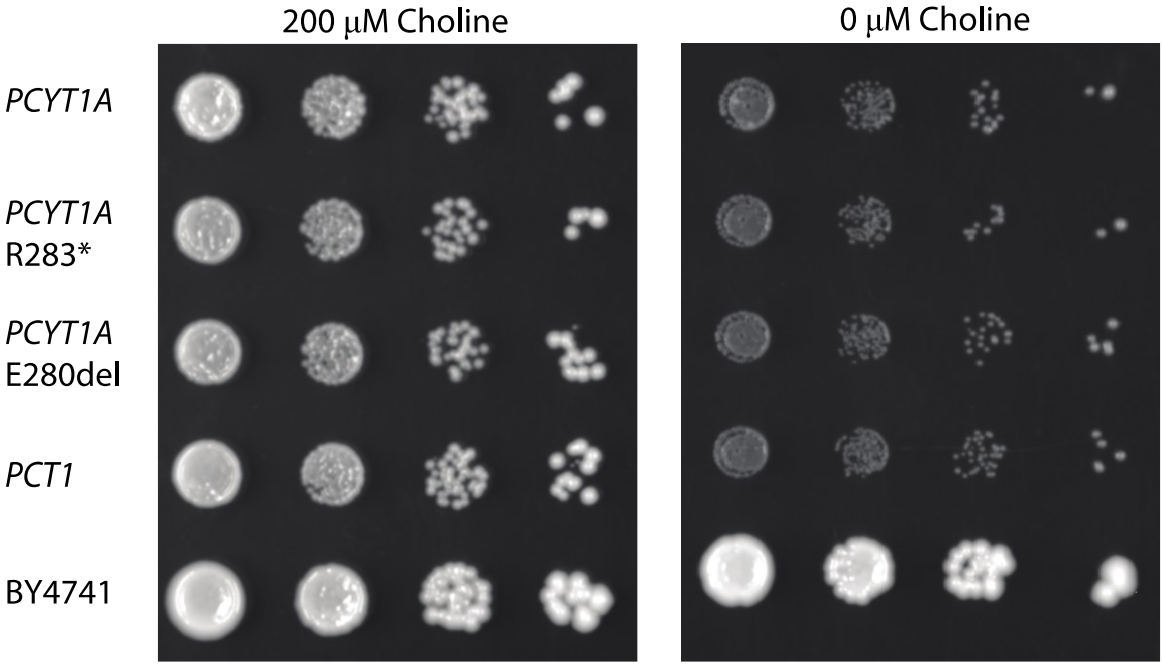

Figure 3.1: **Supplementation with exogenous choline allows growth and survival of haploid yeast cells that are expressing human *PCYT1A* and lack the PE methylation pathway.** Haploid *cho2*Δ *opi3*Δ *pct1*Δ yeast cells that expressed human *PCYT1A* or yeast *PCT1* were grown to mid-log phase and a serial dilution plating assay was performed. Plates were imaged after 3 days of growth at 30°C. BY4741 is a control (wild type) strain that can synthesize PC through the Kennedy pathway and the PE methylation pathway.

mCherry expressed a fusion protein from the PCYT1A C-terminus, thus enabling PCYT1A localization to be visualized in live cells by fluorescence microscopy. Liquid cultures of cells expressing *PCYT1A*-mCherry were grown to mid-log phase in medium not containing choline. Half of the cells were subsequently incubated with 1 mM choline and the cells were visualized using fluorescence microscopy. In the presence of choline PCYT1A-mCherry localized to the nucleoplasm, while in the absence of choline PCYT1A-mCherry localized to the nuclear membrane and ER (Figure 3.2).

These results indicate that human PCYT1A localizes in a similar manner to the known localization of yeast Pct1 in the resting and membrane synthesis stimulated states. This provides further evidence that the expression of human PCYT1A in yeast is a reliable reporter of its activity and function.

3.3 Generating the Disease-Causing Mutations in Human *PCYT1A* in *Saccharomyces cerevisiae*

Mutations in human *PCYT1A* have been reported to be associated with one of three inherited diseases: spondylometaphyseal dysplasia with cone-rod dystrophy (SMD-CRD), Leber congenital amaurosis (LCA), or congenital lipodystrophy with severe fatty liver disease (CL-FLD)[42]. The mutations span three of the four domains of *PCYT1A* (catalytic domain, membrane binding domain, and phosphorylation domain). There does not appear to be a correlation between the location of the mutation and the disease that occurs (Figure 3.3). To study how the mutations affect PCYT1A function, we sought to generate ten of the identified disease-causing mutations using site-directed mutagenesis. These mutations spanned all three *PCYT1A*-mediated inherited diseases.

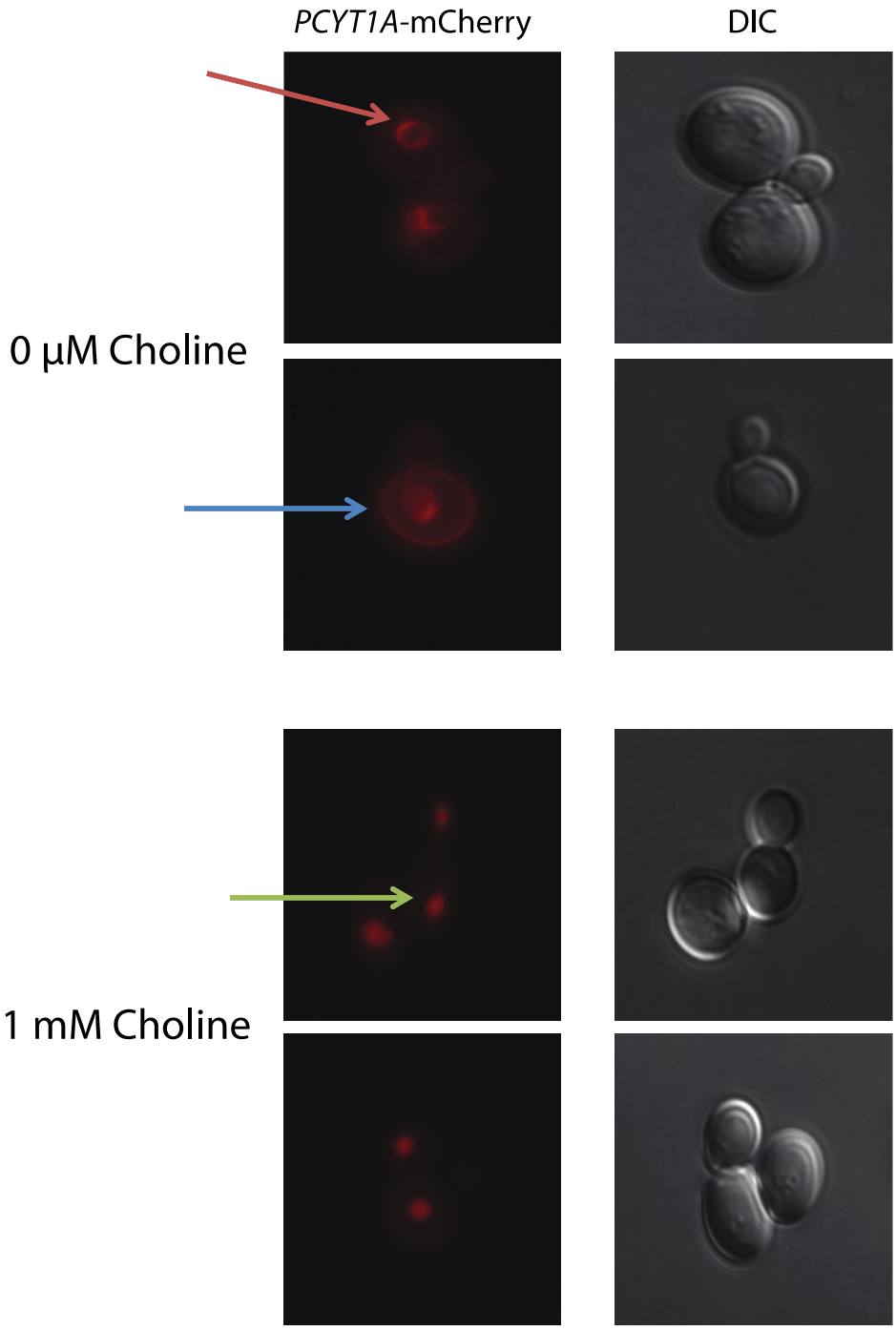

Figure 3.2: **Fluorescence microscopy depicting the localization of human PCYT1A in the presence and absence of choline.** When choline was present in the media, there was localization of the enzyme to the nucleoplasm. When choline was absent from the media, the enzyme localized to the nuclear membrane and ER. The fluorescent tag used was mCherry. A 100x objective with oil was used to visualize the yeast cells. The red arrow points to the nucleus showing nuclear membrane localization, the blue arrow points to the endoplasmic reticulum, and the green arrow points to the nucleus when there is nucleoplasmic localization.

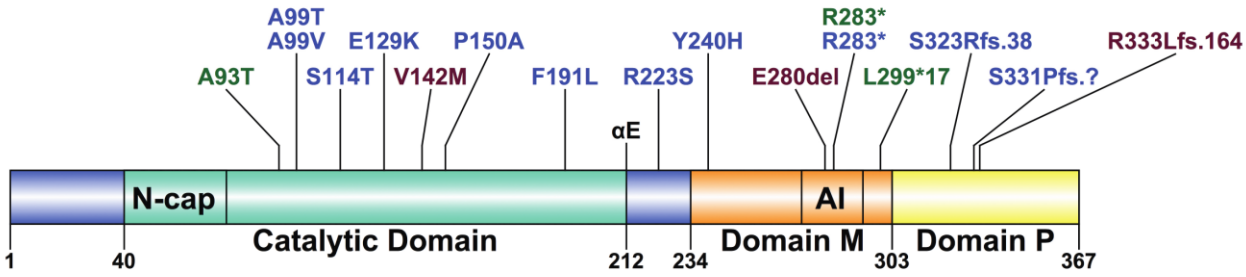

Leber Congenital Amaurosis

Spondylometaphyseal Dysplasia with Cone-Rod Dystrophy

Congenital Lipodystrophy with Severe Fatty Liver Disease

Figure 3.3: **Protein map of human *PCYT1A* denoting the domains and the identified mutations that cause inherited human diseases. "**Fs" denotes a frameshift mutation. "?" denotes a mutation that causes continued translation and is termed a "nonstop" allele. AI denotes the autoinhibitory region.

A plasmid containing the human *PCYT1A* open reading frame was subcloned into the yeast expression vector p416 GPD. Site-directed mutagenesis was performed to create 10 of the mutations observed in the diseases associated with *PCYT1A* mutations. Six of the mutations were linked to SMD-CRD, two were linked to CL-FLD, one was linked to LCA, and one was associated with a combined LCA and SMD-CRD phenotype. The mutations that were generated that are associated with SMD-CRD are all single nucleotide variants (A99T, A99V, E129K, P150A, F191L, R223S). The mutations that were generated and are associated with CL-FLD consist of one single nucleotide variant and a single codon deletion in the autoinhibitory region of the membrane-binding domain (V142M and E280del). The mutation associated with LCA is a single nucleotide variant (A93T) and the mutation associated with both LCA and SMD-CRD is a nonsense mutation (R283*). Each of these mutations was generated using site-directed mutagenesis and their identity was confirmed by DNA sequencing. The resulting plasmids were transformed into a diploid yeast strain heterozygous for *cho2*Δ *opi3*Δ *pct1*Δ. The transformed yeast cells were subjected to random sporulation (forced meiosis) and haploid cells were selected for using nutritional auxotrophies that were present in each inactivated gene, and in the *PCYT1A* expressing plasmid. We ensured that all cells were able to mate to further confirm they were haploid.

Throughout this process, I successfully obtained three individual haploid strains for 9 out of 10 of the *PCYT1A* mutations that we generated. All of these mutations were able to produce viable haploid cells that grew in the presence of choline and did not grow when choline was absent from the media. The V142M mutation did not produce any viable haploid cells. Despite repeated random sporulation attempts, I was unable to

isolate any haploid cells for this mutation. The mutation that I was unable to isolate haploid cells for (V142M) has been studied in an *in vitro* model[42]. In that study, it was found that the V142M mutation caused the protein to completely misfold and it possessed almost no *in vitro* catalytic activity. Our results confirm that the lack of catalytic activity for with this PCYT1A mutant is recapitulated in our yeast expression system for determining PCYT1A function. My results further indicate that 9 of the 10 disease-causing PCYT1A mutations generated are able to produce protein that functions sufficiently to keep cells viable.

3.4 Searching for Differential Phenotypes for *Saccharomyces cerevisiae* Transformed with *PCYT1A* Disease-causing Mutations when Exposed to Cell Stressors

Serial dilution growth assays are a convenient method to probe yeast cells for defects in specific phenotypes depending on the media on which they are grown. These include non-fermentable carbon sources (e.g. glycerol) to probe mitochondrial function/electron transport train activity, use of lipid carbon sources (e.g. oleate) to probe beta-oxidation capacity, determining the capacity to respond to osmotic stress (e.g. sorbitol, NaCl, and KCl), determining the capacity to cope with ER stress (e.g. tunicamycin) or oxidative stress (e.g. Cd^{2+}), the addition of surfactants to probe the ability to respond to membrane perturbation (e.g. sodium dodecyl sulphate (SDS)), and changing growth temperature which can affect membrane fluidity. Specifically, serial dilutions of *cho2*Δ *opi3*Δ *pct1*Δ haploid yeast cells expressing human *PCYT1A* (and mutant variants) grown in liquid culture in standard yeast medium were serial diluted and

then pinned onto various solid media. The media contained either 3% glycerol (substituting for glucose as a carbon source), oleate (substituting for glucose as a carbon source), 1 M sorbitol, 0.4 M KCl, 0.4 M NaCl, 1 μg/mL tunicamycin, 50 μM Cd^{2+}, or 0.01% SDS. The media also contained 200 μM or 5 μM choline for the first set of experiments and 200 μM or 0.5 μM choline for the second set of experiments to further stress cells. Cells were grown for 2-12 days (depending on the media that they were grown on) at 30°C.

When cells were grown at 30°C, we did not see a substantial difference in growth between any of the mutants and wild type *PCYT1A* at 200 μM and 5 μM exogenous choline on normal (SC-ura) yeast media (Figure 3.4). The K_m for the sole choline transporter in yeast, Hnm1, is 0.5 μM[86]. The provision of 5 μM exogenous choline enables a normal rate of cell growth for yeast cells where growth is dependent on human *PCYT1A*, as well as the nine disease-associated *PCYT1A* mutants that I analyzed. When the above cell stressors were added to medium containing either 200 μM or 5 μM exogenous choline, none of the cell stressors appreciably affected cell growth. These experiments were repeated using a dose of 0.5 μM exogenous choline.

3.5 Inositol and Reduced Choline Stress Result in Differential Phenotypes for *PCYT1A* Mutants

In addition to further limiting choline supply to 0.5 μM as a means to search for phenotypes for the *PCYT1A* disease-causing mutants, we also simultaneously limited the exogenous concentration of inositol. Inositol is a master regulator of lipid synthesis in yeast through a complex transcriptional regulatory pathway. High exogenous inositol

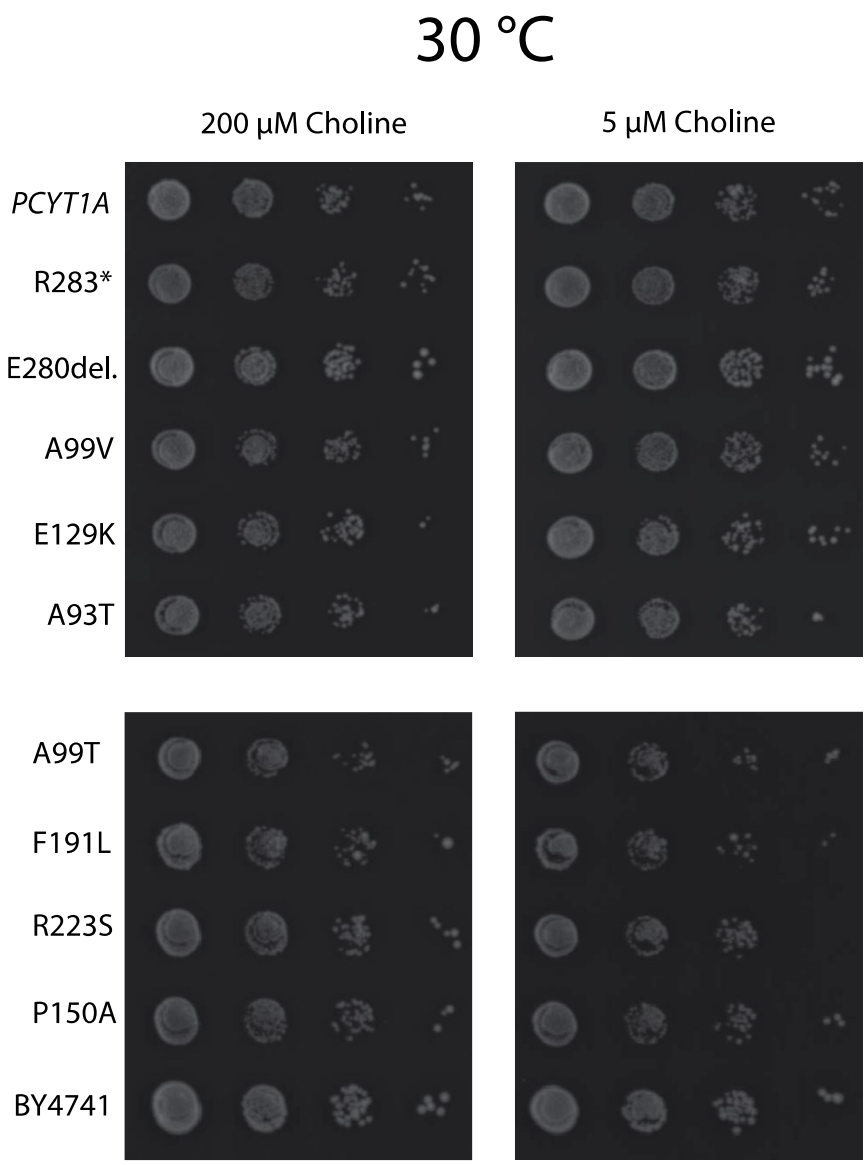

Figure 3.4: **Growth analysis of haploid yeast cells transformed with human *PCYT1A* and the disease-associated mutant variants grown at 30°C with 200 µM or 5 µM choline.** Haploid *cho2*Δ *opi3*Δ *pct1*Δ yeast cells transformed with plasmids were grown to mid-log phase and plated using the serial dilution assay protocol. Plates were imaged after 3 days of growth at 30°C. BY4741 is a control (wild type) strain that contains both *PCT1* and the PE methylation pathway for PC synthesis.

decreases the transcription of almost all phospholipid biosynthetic genes, while low inositol levels increase phospholipid gene transcription[80]. Inositol is normally present in yeast cell medium at 420 μM. We used each of the cell stressors at 200 μM and 0.5 μM choline along with exogenous inositol supplied at 11 μM (low inositol) or no inositol. We determined cell growth for serial diluted yeast onto medium containing either 11 μM inositol or no inositol and determined the effect on cell growth for *cho2*Δ *opi3*Δ *pct1*Δ haploid yeast cells expressing human *PCYT1A* and the mutant variants.

Two conditions resulted in differential growth of *PCYT1A* mutant variants, surfactant and Cd^{2+} addition. Surfactants, such as SDS, report on the ability to respond to cell membrane perturbation[81]. When grown on plates containing SDS, we saw a substantial increase in growth for cells expressing the E280del mutant, and a slight increase in growth for the A99T mutant (Figure 3.5).

Cd^{2+} has been shown to cause oxidative stress leading to toxicity and cell death[82]. The wild type *PCYT1A* expressing cell did not grow well when Cd^{2+} was added to the growth medium. The E280del mutation grew significantly better than the wild type when exposed to this stressor. Many of the other mutations (A99T, F191L, R223S, and P150A) also grew slightly better than the wild type. The A93T mutation grew more poorly when exposed to Cd^{2+} (Figure 3.6).

From the data that was gathered, it appears that there are a few distinct phenotypic trends. Firstly, it appears as though the E280del mutation causes substantially increased growth compared to wild type PCYT1A in the presence of SDS and Cd^{2+}. The A99T mutation also appears to grow better than the wild type on media containing either of these stressors. Many *PCYT1A* patient-derived mutations grew better than wild type on

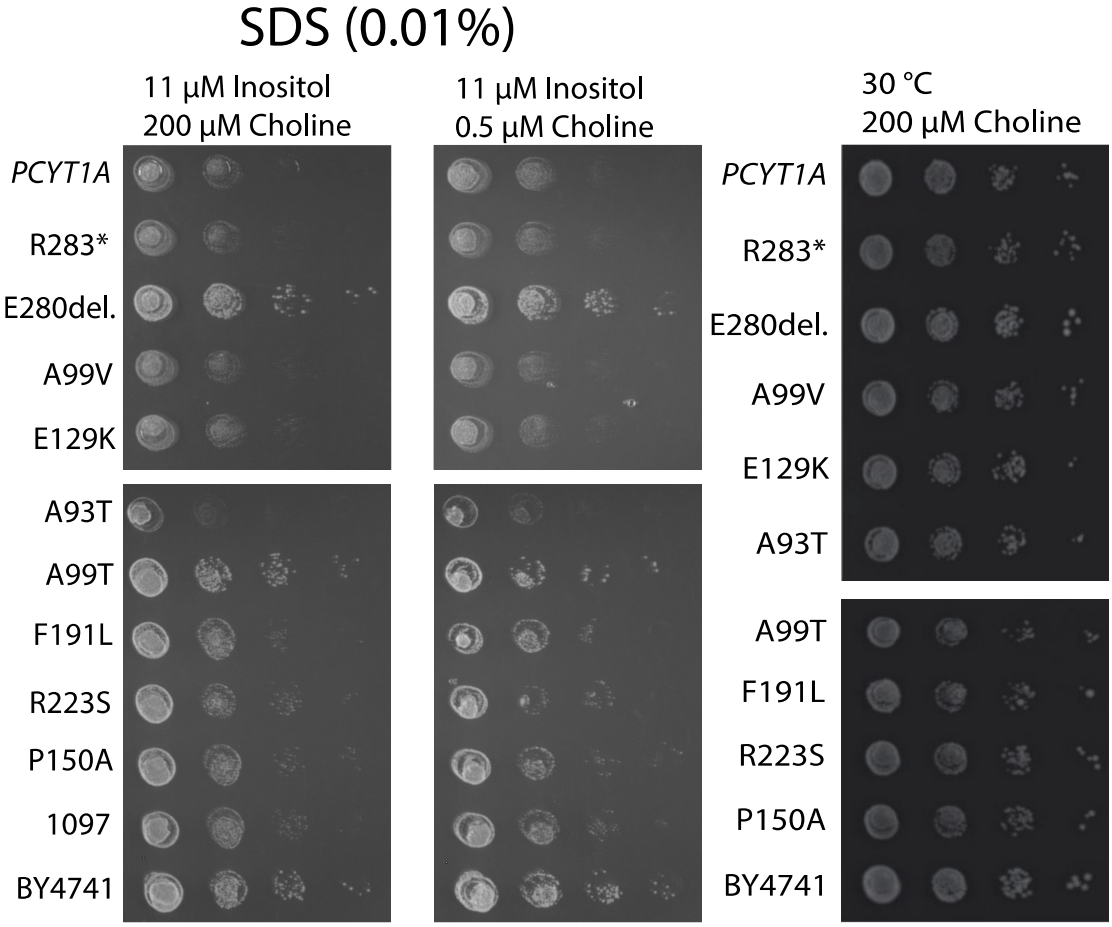

Figure 3.5: **Growth analysis of haploid yeast cells transformed with human *PCYT1A* and the disease-associated mutant variants of the gene grown in the presence of 0.01% sodium dodecyl sulphate, 200 µM or 0.5 µM choline, and 11 µM inositol.** Haploid *cho2*Δ *opi3*Δ *pct1*Δ yeast cells transformed with plasmids were grown to mid-log phase and plated using the serial dilution assay protocol. Plates were imaged after 3 days of growth at 30°C. BY4741 is a control (wild type) strain that contains both *PCT1* and the PE methylation pathway for PC synthesis.

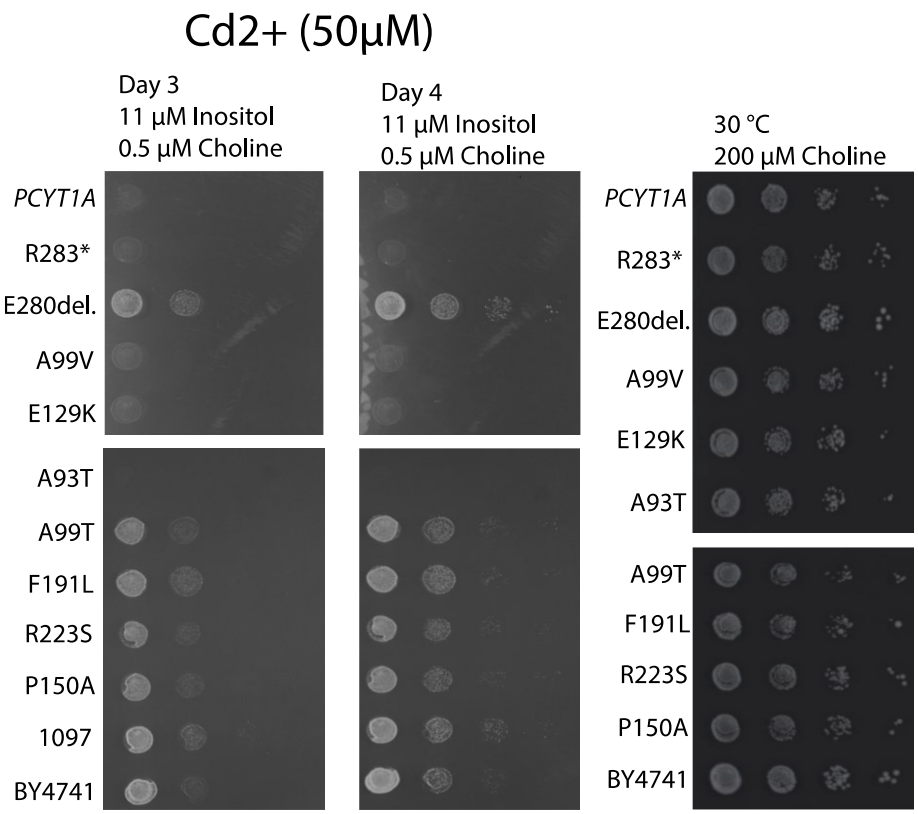

Figure 3.6: **Growth analysis of haploid yeast cells transformed with human *PCYT1A* and the disease-associated mutant variants of the gene grown in the presence of 50 μM Cd^{2+}, 200 μM or 0.5 μM choline, and 11 μM inositol.** Haploid *cho2*Δ *opi3*Δ *pct1*Δ yeast cells transformed with our plasmids were grown to mid-log phase and plated using the serial dilution assay protocol. Plates were imaged after 3 and 4 days of growth at 30°C. BY4741 denotes a control strain that contains both *PCT1* and the PE methylation pathway for PC synthesis.

medium containing Cd^{2+}. Lastly, the A93T mutation appears to hinder growth slightly on Cd^{2+}-containing medium.

3.6 A Novel Patient-derived *EPT1* Mutation Reduces PE Synthesis via the CDP-Ethanolamine Pathway

The Kennedy pathway possesses two branches: the CDP-choline branch that is responsible for the synthesis of PC, and the CDP-ethanolamine branch that is responsible for the synthesis of PE. Mutations in *EPT1* have been shown to cause an inherited spastic paraplegia[70]. A new point mutation in *EPT1* in a spastic paraplegia patient, resulting in a P45L amino acid change, was identified. I sought to determine if this mutation has an effect on the synthesis of PE.

To determine if the P45L mutation in human *EPT1* has an effect on PE synthesis via the CDP-ethanolamine pathway, wild type and mutant human *EPT1* were subcloned into the p416 GPD yeast expression vector. The resulting constructs were expressed in a yeast strain lacking the endogenous *EPT1* gene. Liquid cultures of the cells were grown to mid-log phase and washed with ammonium sulphate-free media. The cultures were labeled with [^{14}C]ethanolamine and incubated for 1 hour. The addition of radiolabelled ethanolamine allowed us to measure the biosynthesis of PE. Upon termination of radiolabelling, cell extracts were separated using thin layer chromatography and the radiolabel associated with ethanolamine, phosphoethanolamine, CDP-ethanolamine, PE, and PC (PE can be converted to PC in this strain by the PE methylation pathway) was determined using a liquid scintillation counter. A western blot was performed and

determined that wild type EPT1 and the mutant version were expressed at the same level (Figure 3.7B).

We observed differences in radiolabel in yeast expressing the wild type human *EPT1* and the P45L mutant variant of human *EPT1*. There was a 2-fold increase in the amount of radiolabelled CDP-ethanolamine as well as increases in radiolabel in its upstream metabolites, ethanolamine and phosphoethanolamine (Figure 3.7C). There was also a 2-fold decrease in the amount of PE, and its downstream metabolite, PC. Significance of the data was determined using an unpaired Student's t-test and error bars were generated using the standard error.

These experiments determined that the mutation identified in *EPT1* in patients with complex hereditary spastic paraplegia causes a decrease in EPT1 activity. This leads to a build-up of its substrate, CDP-ethanolamine, and the upstream metabolites, ethanolamine and phosphoethanolamine, and a decrease in labeling of its product, PE, and its downstream metabolite, PC.

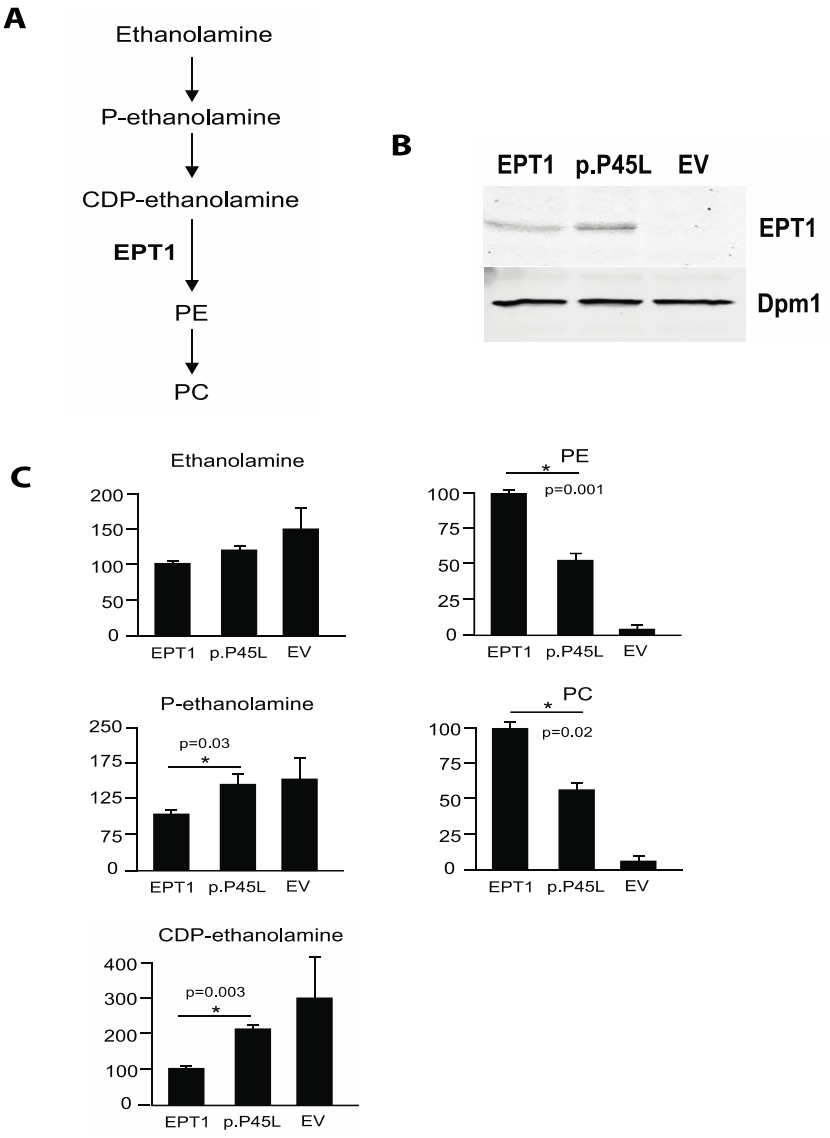

Figure 3.7: **The Effect of the Patient-Derived P45L Mutation on Human EPT1 Activity.** A. Overview of the CDP-ethanolamine pathway. EPT1 catalyzes the conversion of CDP-ethanolamine to phosphatidylethanolamine. B. Western blot depicting that the expression of the P45L mutant is not less than the expression of wild-type EPT1 in yeast. C. Graphic representation of the results from metabolic radiolabeling of the CDP-ethanolamine pathway. The y-axis represents the mean % of wild type radioactive counts. The error bars were generated by calculating the standard error using a sample size of 4. The test used to determine statistical significance was an unpaired Student's t-test. The P45L mutation caused a 2-fold increase in the amount of CDP-ethanolamine compared to wild-type EPT1 as well as increases in the other upstream metabolites, phosphoethanolamine and ethanolamine. The P45L mutation also caused a 2-fold decrease in the amount of PE and its downstream metabolite, PC, compared to wild-type EPT1.

CHAPTER 4: DISCUSSION

The work presented in this thesis is part of an ongoing study of how mutations in genes in the Kennedy pathway can be associated with different inherited diseases. To gather the results presented in this thesis, I used *Saccharomyces cerevisiae* as a model organism to study the function of two important human proteins involved in the Kennedy pathway that contained inherited disease-associated mutations. Yeast has been used in various studies for the characterization of human phospholipid biosynthesis, but it has not been previously shown that human PCYT1A can function in place of the yeast version of the enzyme, Pct1[51,77,78]. PCYT1A is the rate-limiting enzyme in the CDP-choline branch of the Kennedy pathway in humans and although three distinct diseases have been linked to mutations in the gene, how they affect the function of the enzyme is largely unknown[9,42]. In this work, I sought to use yeast as a model organism to study how mutations in human *PCYT1A* can be linked to SMD-CRD, LCA, or CLD-FLD. Through my research, I determined that yeast can be used as a model organism to study human *PCYT1A* in the absence of yeast *PCT1*. Human PCYT1A also localizes in yeast in a similar manner as has been reported in mammalian cells. Some of the disease-associated mutations in human *PCYT1A* show distinct growth phenotypes when exposed to cell stressors. While studying the CDP-ethanolamine pathway and the new P45L patient-derived mutation in human *EPT1*, using metabolic radiolabelling I determined that this mutation causes a decrease in EPT1 activity.

4.1 *PCYT1A* and Yeast Survival

Yeast has been used in various studies in the past to characterize enzymes involved with phospholipid synthesis. Prior to my study, *PCYT1A* had yet to be studied in great detail using yeast as a model organism. I sought to use yeast as a model organism to better understand the inherited disease-causing mutations in human *PCYT1A* and how they affect PC synthesis, and to uncover more information about how these inherited diseases may be caused.

Since yeast cells, under normal conditions, synthesize PC through both the CDP-choline and PE methylation pathway, I needed to restrict cells from synthesizing PC through the PE methylation pathway by inactivating the *CHO2* and *OPI3* genes[79,83]. To determine if human PCYT1A is able to replace Pct1 function in *S. cerevisiae*, I transformed yeast cells with a plasmid expressing human PCYT1A in a *cho2*Δ *opi3*Δ *pct1*Δ strain that is unable to synthesize PC through the PE methylation or CDP-choline pathway. This haploid strain was obtained from random sporulation (forced meiosis of heterozygous diploids) and the resulting haploid cells would rely entirely on the human protein generated by *PCYT1A* for viability.

Choline is the precursor for PC synthesis through the CDP-choline pathway and yeast cells require choline uptake from their surroundings as they cannot synthesize this nutrient *de novo*[84,85]. This means that without choline in the media, yeast cells dependent on the CDP-choline pathway for life would be unable to synthesize PC and would not be able to grow. I was able to verify that PCYT1A was indeed keeping the *cho2*Δ *opi3*Δ *pct1*Δ haploid yeast cells viable by synthesizing PC through the CDP-choline pathway as in the presence of choline, haploid *cho2*Δ *opi3*Δ *pct1*Δ cells expressing wild type

PCYT1A were viable, while in the absence of choline they did not grow. From these results, I determined that human PCYT1A can replace the essential activity of yeast Pct1 in *Saccharomyces cerevisiae.*

4.2 *PCYT1A* Localization in Yeast

PCYT1A has been shown in mammalian cells to localize to the peripheral ER/nuclear membrane when catalytically active, and localizes to the nucleoplasm and the cytoplasm (in some cell types) when catalytically inactive[9]. We sought to determine if human *PCYT1A* localizes in yeast cells in the same manner that it has been reported to localize in mammalian cells.

In order to study this, a plasmid expressing wild type *PCYT1A* was transformed into a yeast strain that was not deficient in PC synthesis (meaning it could synthesize PC through the CDP-choline pathway and the PE methylation pathway). The plasmid enabled tagging of the PCYT1A coding sequence with mCherry. This allowed us to study the localization of the protein using fluorescence microscopy in live cells. The addition and removal of choline were used to study how the protein localized when it was catalytically active versus catalytically inactive.

We determined that when there was choline present in the media, PCYT1A localized to the nucleoplasm (as under these conditions, it was catalytically inactive). When we removed choline from the media, we saw that the protein localized to the peripheral ER and nuclear membrane. This is similar to what has been reported for the localization of active PCYT1A in mammalian cells[38]. Also, it has been shown that yeast Pct1 localizes from the nucleoplasm to the nuclear membrane/ER when the media is

lacking in choline and PC synthesis is required. Expression of human PCYT1A protein in yeast resulted in a similar pattern of localization upon the addition of choline to both PCYT1A expression in mammalian cells, and Pct1 expression in yeast. This implies that the major form of regulation of human PCYT1A activity is intact when expressed in yeast cells.

4.3 Mutations in *PCYT1A* Affect Yeast Growth

To study the disease-associated mutations in *PCYT1A* in our system, mutations were generated using site-directed mutagenesis and the resulting DNA fragments were subcloned into a yeast expression vector. This plasmid was transformed into a yeast strain that was deficient in PC synthesis and the cells were forced to undergo meiosis to generate a *cho2*Δ *opi3*Δ *pct1*Δ haploid strain. These strains would be dependent on the expressed mutant PCYT1A protein for growth, and growth would be choline dependent. The haploid cells were further surveyed for any growth phenotypes using a serial dilution pinning assay and various known cell stressors. Interestingly, of the ten disease-causing *PCYT1A* mutations tested, nine resulted in normal growth in the presence of choline in regular yeast medium. This implies that there is enough catalytic activity present in each mutant to enable normal cell growth.

4.3.1 PCYT1A E280del

The E280del in *PCYT1A* is associated with CLD-FLD[47]. In previous studies from the Cornell lab, it was shown using purified enzyme from COS-1 cells that the E280del mutation in *PCYT1A* causes instability in the folding of just the catalytic domain[42]. This

mutation is a single codon deletion that occurs in the auto-inhibitory helix in the membrane-binding domain. From this study, it was also shown that when exposed to anionic lipid vesicles (to activate the enzyme) *in vitro*, there was a 4-fold increase in the amount of enzyme activity when there was no lipid present. This mutation increased the response to these lipid vesicles 4-fold as well[42].

The results that we saw indicated that across various conditions the E280del mutation seemed to grow much more than the wild type *PCYT1A*-expressing cells. We saw this especially when we exposed the cells to 0.01% SDS and 50 μM Cd^{2+}, even when choline concentrations were low. These results were surprising as there have been studies completed using EBV-transformed lymphocytes and skin fibroblasts from two patients and in each case, *PCYT1A* expression was incredibly low and PC synthesis was severely reduced[47]. The results that this group observed could be due to the fact that they were looking at the compound heterozygous mutations that are present in patients as opposed to looking at an isolated mutation in *PCYT1A*. Since I did see increased growth compared to the wild type-expressing cells even under most stress-inducing conditions with the E280del mutation, I believe that my results may be in line with what the Cornell lab observed. The E280del mutation may be affecting how the auto-inhibitory helices are folding to prevent access to the catalytic core by the substrate. This could in-turn cause an increase in the activity of the enzyme and potentially cause it to be catalytically active when it is not membrane bound. Something that will be important for future studies to check is that the expression level of the E280del mutant variant is similar to the wild type in our model. This could be done by performing a western blot to measure any

differences in protein expression between the wild type PCYT1A and the E280del mutant variant.

4.3.2 PCYT1A p.A93T

The A93T mutation in *PCYT1A* is associated with LCA, which is an isolated retinal dystrophy[46]. The aforementioned study that emerged from the Cornell lab also used COS-1 cells to purify PCYT1A that possessed this mutation. What they determined for the A93T mutation is that the catalytic activity was impaired as this mutation occurs in the catalytic core[42]. They also observed some misfolding of the protein that caused reduced solubility.

From our results, we saw that in the presence of 50 μM Cd^{2+} that this particular mutation grew more poorly than the wild type. Due to the misfolding and decreased enzyme activity that was observed in the *in vitro* studies performed by the Cornell lab, it makes sense that we saw a decrease in growth in relation to this mutation. Cd^{2+} is a heavy metal that is toxic to cells in high concentrations via a plethora of intracellular effects related to oxidative stress. More studies will be required to determine why the A93T mutation is specifically sensitive to Cd^{2+} exposure.

4.3.3 PCYT1A p.A99T

The A99T mutation in *PCYT1A* is associated with SMD-CRD, a cone-rod dystrophy that presents alongside short stature and bone deformation[39]. The Cornell lab also studied this mutation expressed in COS-1 cells and using purified protein, they found that similarly to the A93T mutation, the A99T mutation caused a decrease in catalytic

activity[42]. This protein, when isolated, was found to be present in the soluble fraction and not the particulate fraction implying that it was mainly in its inactive form.

From our results, we saw that in the presence of 50 μM Cd^{2+} and 0.01% SDS the A99T mutation seemed to grow slightly better than the wild type protein. This was surprising as the mutation is in the catalytic core, similarly to the A93T mutation. For this mutation it would be greatly beneficial to measure the protein expression levels and compare them to the wild type using a Western blot. If the expression levels are significantly higher, perhaps that is leading to the slightly increased growth that we are observing with this mutation. The results from the Cornell lab indicate that this mutation causes slightly decreased enzyme activity, but our results showing increased growth are somewhat contradictory.

4.3.4 PCYT1A p.V142M

The V142M mutation in *PCYT1A* is associated with CLD-FLD[47]. The Cornell lab attempted to study this mutation *in vitro*, but they were not successful in isolating and purifying the protein. This is because they discovered that this mutation causes complete misfolding of PCYT1A and an enzyme activity that was barely detectable over baseline levels[42]. Since the V142 residue is conserved across all CCTs, it is likely that a mutation at this location causes the enzyme to be non-functional.

When I attempted to perform random sporulation with this particular mutation, I was unsuccessful in isolating any haploid cells. This is likely because the enzyme is essentially catalytically inactive due to complete misfolding and the yeast cells were unable to use this protein to synthesize PC. Since the yeast strain that we used was able to

synthesize PC via the PE methylation pathway when it was diploid, the cells were viable in the diploid state. During random sporulation, it is likely that all of the cells that were haploid and lacked the ability to synthesize PC through the PE methylation pathway and CDP-choline pathway. These cells then died due to a lack of functioning PCYT1A protein and an absence of PC synthesis.

4.4 The Effect of a Novel Patient-Derived *EPT1* Mutation on PE Synthesis

As mentioned previously, yeast has been used for many studies on the phospholipid biosynthesis pathways that are present in eukaryotic cells. Human *EPT1* and some of its disease-associated mutations have previously been studied and characterized by members of our lab and it was found that a patient-derived mutation (R112P) in *EPT1* caused a decrease in enzyme activity consistent with a loss-of-function mutation[21]. A novel patient-derived mutation (P45L) had been recently identified and we sought to study it to determine the effect of this mutation on EPT1 activity and PE synthesis via the CDP-ethanolamine pathway.

To study this mutation, the mutant variant of *EPT1* (P45L) was generated using site-directed mutagenesis and subcloned into a yeast expression vector. We then transformed a strain of yeast lacking the endogenous *EPT1* with human *EPT1* and the P45L mutant variant. We then used [^{14}C]ethanolamine to determine if the biosynthesis of PE is affected by this mutation.

From the data generated, we saw that there was a 2-fold increase in the amount of radiolabeled CDP-ethanolamine and an increase in its upstream metabolites. We also observed that there was a 2-fold decrease in the amount of PE and its downstream

metabolite, PC. This mutation is obviously affecting the activity of EPT1 and causes at least partial loss-of-function. Since HSP is a neurological disorder and PE is such an important phospholipid in the brain, the decrease in enzyme activity of EPT1 with this mutation may be leading to the disease through the decreased PE synthesis from the CDP-ethanolamine pathway[20].

CHAPTER 5: CONCLUSIONS AND FUTURE DIRECTIONS

The work presented in this thesis has furthered our understanding in how patient-derived mutations in human *EPT1* and *PCYT1A* can be associated with human diseases, but there is still much to be uncovered. While we know that some mutations in *PCYT1A* cause a distinct growth phenotype when exposed to certain cell stressors, we do not know exactly how the growth phenotype is being caused. In order to further study this, firstly western blots should be performed to ensure that protein expression is similar across all of the generated mutants. Then, metabolic radiolabelling of the CDP-choline pathway using [^{14}C]choline could be performed to see if there are differences in the biosynthesis of PC between the wild type and mutant enzymes.

The preliminary results for the serial dilution pinning assays show that some mutant variants of human *PCYT1A* cause distinct phenotypes when exposed to known cell stressors, but further replicates are required to confirm these findings. The replicates can be done using all three isolated strains for each mutant variant to confirm that the phenotypes are consistent and not the result of a genetic event that occurred during the construction of that strain.

While tissue-specific knockouts of *PCYT1A* have been studied in mice, the effects of the patient-derived mutations have yet to be studied in an animal model. Most of the data regarding the effects of *PCYT1A* mutations comes from initial studies using patient fibroblasts and/or *in vitro* enzyme activity studies. Using more complex model organisms such as mice or zebrafish could lead to a greater understanding of how these mutations are leading to the associated inherited diseases. Specifically, I think that it would be beneficial to study the E280del mutation in *PCYT1A* in mice. The severe fatty liver

disease that occurs may be linked to an upregulation in the PE methylation pathway that occurs only in hepatocytes in mammals. This could perhaps explain the fatty liver symptom that occurs with this disease.

Something that is important to note is that although all of the diseases are recessive, most of the patients are compound heterozygous. This means that there is a difference mutation present on each allele. This is especially important to recognize as PCYT1A dimerizes and this dimerization is essential for catalytic activity. This was one of the major limitations of our study as we were able to determine how singular PCYT1A mutations affect the growth of yeast when exposed to cell known cell stressors, but we did not query how two mutations present in the same cell affect PCYT1A function. In order to study the cause of these diseases more in-depth, it will be important in future studies to look at the effect of the different combinations of compound heterozygous mutations reported in proteins both *in vitro* and in model organisms.

References

1. Boycott, K.M., Vanstone, M.R., Bulman, D.E. & MacKenzie, A.E. Rare-disease genetics in the era of next-generation sequencing: discovery to translation. *Nature Reviews. Genetics* **14(10)**, 681-691 (2013).

2. Posey, J.E. Genome sequencing and implications for rare disorders. *Orphanet Journal of Rare Diseases* **14(1)**, 153 (2019).

3. Boycott, K.M., Dyment, D.A., Sawyer, S.L., Vanstone, M.R. & Beaulieu, C.L. Identification of Genes for Childhood Heritable Diseases. *Annual Review of Medicine* **65**, 19-31 (2014).

4. Wetterstrand, K.A. The Cost of Sequencing a Human Genome. (National Human Genome Research Institute, 2019).

5. Veltman, J.A. & Brunner, H.G. De novo mutations in human genetic disease. *Nature Reviews. Genetics* **13(8)**, 565-575 (2012).

6. Fagone, P. & Jackowski, S. Membrane phospholipid synthesis and endoplasmic reticulum function. *Journal of Lipid Research* **50(Supplement)**, S311-S316 (2009).

7. Fajardo, V.A., McMeekin, L. & LeBlanc, P.J. Influence of Phospholipid Species on Membrane Fluidity: A Meta-analysis for a Novel Phospholipid Fluidity Index. *The Journal of Membrane Biology* **244(2)**, 97-103 (2011).

8. Fagone, P. & Jackowski, S. Phosphatidylcholine and the CDP–choline cycle. *Biochimica et Biophysica Acta (BBA)-Molecular and Cell Biology of Lipids* **1831(3)**, 523-532 (2013).

9. McMaster, C.R. From yeast to humans – roles of the Kennedy pathway for phosphatidylcholine synthesis. *FEBS letters* **592(8)**, 1256-1272 (2018).

10. Rawicz, W., Olbrich, K.C., McIntosh, T., Needham, D. & Evans, E. Effect of Chain Length and Unsaturation on Elasticity of Lipid Bilayers. *Biophysical journal* **79(1)**, 328-339 (2000).

11. Agassandian, M. & Mallampalli, R.K. Surfactant phospholipid metabolism. *Biochimica et Biophysica Acta (BBA)-Molecular and Cell Biology of Lipids* **1831(3)**, 612-625 (2014).

12. DeLong, C.J., Shen, Y.-J., Thomas, M.J. & Cui, Z. Molecular Distinction of Phosphatidylcholine Synthesis between the CDP-Choline Pathway and Phosphatidylethanolamine Methylation Pathway. *Journal of Biological Chemistry* **274(42)**, 29683-29688 (1999).

13. Rader, D.J., Alexander, E.T., Weibel, G.L., Billheimer, J. & Rothblat, G.H. The role of reverse cholesterol transport in animals and humans and relationship to atherosclerosis. *Journal of Lipid Research* **50(Supplement)**, S189-S194 (2009).

14. Tchoua, U., Gillard, B.K. & Pownall, H.J. HDL superphospholipidation enhances key steps in reverse cholesterol transport. **209(2)**, 430-435 (2010).

15. Shamburek, R.D., Zech, L.A., Cooper, P.S., Vandenbroek, J.M. & Schwartz, C.C. Disappearance of two major phosphatidylcholines from plasma is predominantly via LCAT and hepatic lipase *American Journal of Physiology-Endocrinology and Metabolism* **271(6)**, E1073-E1082 (1996).

16. Gibbons, G.F., Wiggins, D., Brown, A.-M. & Hebbachi, A.-M. Synthesis and function of hepatic very-low-density lipoprotein. *Biochemical Society Transactions* **32(1)**, 59-64 (2004).

17. JN, v.d.V. *et al.* The critical role of phosphatidylcholine and phosphatidylethanolamine metabolism in health and disease. *Biochimica et Biophysica Acta* **1859**, 1558-1572 (2017).

18. Furse, S. & De Kroon, A.I. Phosphatidylcholine's functions beyond that of a membrane brick. *Molecular membrane biology* **32(4)**, 117-119 (2015).

19. Dawaliby, R. *et al.* Phosphatidylethanolamine Is a Key Regulator of Membrane Fluidity in Eukaryotic Cells. *Journal of Biological Chemistry* **291(7)**, 3658-3667 (2016).

20. Vance, J.E. & Tasseva, G. Formation and function of phosphatidylserine and phosphatidylethanolamine in mammalian cells. *Biochimica et Biophysica Acta (BBA)-Molecular and Cell Biology of Lipids* **1831(3)**, 543-554 (2012).

21. Hishikawa, D., Hashidate, T., Shimizu, T. & Shindou, H. Diversity and function of membrane glycerophospholipids generated by the remodeling pathway in mammalian cells. *Journal of Lipid Research* **55(5)**, 799-807 (2014).

22. Siegel, D.P. & Epand, R.M. The mechanism of lamellar-to-inverted hexagonal phase transitions in phosphatidylethanolamine: implications for membrane fusion mechanisms. *Biophysical journal* **73(6)**, 3089-3111 (1997).

23. Zeisel, S.H. Dietary choline: biochemistry, physiology, and pharmacology. *Annual review of nutrition* **1(1)**, 95-121 (1981).

24. Snider, S.A. *et al.* Choline transport links macrophage phospholipid metabolism and inflammation. *Journal of Biological Chemistry* **293(29)**, 11600-11611 (2018).

25. Michel, V., Yuan, Z., Ramsubir, S. & Bakovic, M. Choline Transport for Phospholipid Synthesis. *Experimental Biology and Medicine* **231(5)**, 490-504 (2006).

26. Hedtke, V. & Bakovic, M. Choline transport for phospholipid synthesis: An emerging role of choline transporter-like protein 1. *Experimental Biology and Medicine* **244(8)**, 655-662 (2019).

27. Schenkel, L.C. *et al.* Mechanism of choline deficiency and membrane alteration in postural orthostatic tachycardia syndrome primary skin fibroblasts. *The FASEB Journal* **29(5)**, 1663-1675 (2015).

28. Yuan, Z., Tie, A., Tarnopolsky, M. & Bakovic, M. Genomic organization, promoter activity, and expression of the human choline transporter-like protein 1. *Physiological genomics* **26(1)**, 76-90 (2006).

29. Aoyama, C., Liao, H. & Ishidate, K. Structure and function of choline kinase isoforms in mammalian cells. *Progress in lipid research* **43(3)**, 266-281 (2004).

30. Gruber, J. *et al.* Balance of human choline kinase isoforms is critical for cell cycle regulation. *The FEBS journal* **279(11)**, 1915-1928 (2012).

31. Wu, G., Aoyama, C., Young, S.G. & Vance, D.E. Early Embryonic Lethality Caused by Disruption of the Gene for Choline Kinase α, the First Enzyme in Phosphatidylcholine Biosynthesis. *Journal of Biological Chemistry* **283(3)**, 1456-1462 (2008).

32. Li, Z. *et al.* Choline kinase beta is required for normal endochondral bone formation. *Biochimica et Biophysica Acta (BBA)-General Subjects* **1840(7)**, 2112-2122 (2014).

33. Mitsuhashi, S. & Nishino, I. Megaconial congenital muscular dystrophy due to loss-of-function mutations in choline kinase β. *Current Opinion in Neurology* **26(5)**, 536-543 (2013).

34. Mitsuhashi, S. *et al.* A Congenital Muscular Dystrophy with Mitochondrial Structural Abnormalities Caused by Defective De Novo Phosphatidylcholine Biosynthesis. *The American Journal of Human Genetics* **88(6)**, 845-851 (2011).

35. Molina, A.R.r.d. *et al.* Overexpression of choline kinase is a frequent feature in human tumor-derived cell lines and in lung, prostate, and colorectal human cancers. *Biochemical and biophysical research communications* **296(3)**, 580-583 (2002).

36. Karim, M., Jackson, P. & Jackowski, S. Gene structure, expression and identification of a new CTP: phosphocholine cytidylyltransferase β isoform. *Biochimica et Biophysica Acta (BBA)-Molecular and Cell Biology of Lipids* **1633(1)**, 1-12 (2013).

37. Wang, Y., Sweitzerz, T.D., Weinhold, P.A. & Kent, C. Nuclear Localization of Soluble CTP:Phosphocholine Cytidylyltransferase. *Journal of Biological Chemistry* **268(8)**, 5899-5904 (1993).

38. Yao, Z.M., Jamil, H. & Vance, D.E. Choline Deficiency Causes Translocation of CTP:Phosphocholine Cytidylyltransferase from Cytosol to Endoplasmic Reticulum in Rat Liver *Journal of Biological Chemistry* **265(8)**, 4326-4331 (1990).

39. Jurgens, J. *et al.* Loss of function variants in PCYT1A causing spondylometaphyseal dysplasia with cone/rod dystrophy have broad consequences on lipid metabolism, chondrocyte differentiation, and lipid droplet formation. *bioRxiv*. (2019).

40. Kent, C. CTP:phosphocholine cytidylyltransferase. *Biochimica et Biophysica Acta (BBA) - Lipids and Lipid Metabolism* **1348(1-2)**, 79-90 (1997).

41. Cornell, R. Chemical Cross-linking Reveals a Dimeric Structure for CTP:Phosphocholine Cytidylyltransferase. *Journal of Biological Chemistry* **264(15)**, 9077-9082 (1988).

42. Cornell, R.B. *et al.* Disease-linked mutations in the phosphatidylcholine regulatory enzyme CCTα impair enzymatic activity and fold stability. *Journal of Biological Chemistry* **294(5)**, 1490-1501 (2018).

43. Johnson, J.E. & Cornell, R.B. Amphitropic proteins: regulation by reversible membrane interactions. *Molecular membrane biology* **16(3)**, 217-235 (2009).

44. Wang, L., Magdaleno, S., Tabas, I. & Jackowski, S. Early Embryonic Lethality in Mice with Targeted Deletion of the CTP:Phosphocholine Cytidylyltransferase Gene (Pcyt1a). *Molecular and cellular biology* **25(8)**, 3357-3363 (2005).

45. Gunter, C. *et al.* Probucol therapy overcomes the reproductive defect in CTP: phosphocholine cytidylyltransferase β2 knockout mice. *Biochimica et Biophysica Acta (BBA)-Molecular and Cell Biology of Lipids* **1771(7)**, 845-852 (2007).

46. Testa, F. *et al.* Mutations in the PCYT1A gene are responsible for isolated forms of retinal dystrophy. *European Journal of Human Genetics* **25(5)**, 651-655 (2017).

47. Payne, F. *et al.* Mutations disrupting the Kennedy phosphatidylcholine pathway in humans with congenital lipodystrophy and fatty liver disease. *Proceedings of the National Academy of Sciences* **111(24)**, 8901-8906 (2014).

48. Hoover-Fong, J. *et al.* Mutations in PCYT1A, Encoding a Key Regulator of Phosphatidylcholine Metabolism, Cause Spondylometaphyseal Dysplasia with Cone-Rod Dystrophy. *The American Journal of Human Genetics* **94(1)**, 105-112 (2014).

49. Wong, C.K. Novel mutations in PCYT1A are responsible for spondylometaphysealdysplasia with cone-rod dystrophy. *Clinical genetics* **85(6)**, 532-533 (2014).

50. McMaster, C.R. & Bell, R.M. CDP-choline: 1, 2-diacylglycerol cholinephosphotransferase. *Biochimica et Biophysica Acta (BBA)-Lipids and Lipid Metabolism* **1348(1-2)**, 100-110 (1997).

51. Henneberry, A.L., Wistow, G. & McMaster, C.R. Cloning, genomic organization, and characterization of a human cholinephosphotransferase. *Journal of Biological Chemistry* **275(38)**, 29808-29815 (2000).

52. Cornell, R. Cholinephosphotransferase from mammalian sources. *Methods in enzymology* **209**, 267-272 (1992).

53. Funai, K. *et al.* Skeletal muscle phospholipid metabolism regulates insulin sensitivity and contractile function. *Diabetes* **65(2)**, 358-370 (2016).

54. Sundler, R. & Akesson., B. Regulation of phospholipid biosynthesis in isolated rat hepatocytes. Effect of different substrates. *Journal of Biological Chemistry* **250(9)**, 3359-3367 (1975).

55. Verkade, H.J. *et al.* N-methyltransferase pathway is quantitatively not essential for biliary phosphatidylcholine secretion. *Journal of Lipid Research* **48(9)**, 2058-2064 (2007).

56. Watanabe, M. *et al.* Pemt Deficiency Ameliorates Endoplasmic Reticulum Stress in Diabetic Nephropathy. *PloS one* **9(3)**, e92647 (2014).

57. Vance, D.E. & Walkey, C.J. Roles for the methylation of phosphatidylethanolamine. *Current opinion in lipidology* **9(2)**, 125-130 (1998).

58. Yorek, M.A., Rosario, R.T., Dudley, D.T. & Spector, A.A. The utilization of ethanolamine and serine for ethanolamine phosphoglyceride synthesis by human Y79 retinoblastoma cell. *260(5)*, 2930-2936 (1985).

59. Infante, J.P. Rate-limiting steps in the cytidine pathway for the synthesis of phosphatidylcholine and phosphatidylethanolamine. *Biochemical Journal* **167(3)**, 847-849 (1977).

60. Houweling, M., Tijburg, L.B.M., Vaartjes, W.J. & Van Golde, L.M.G. Phosphatidylethanolamine metabolism in rat liver after partial hepatectomy. Control of biosynthesis of phosphatidylethanolamine by the availability of ethanolamine. *Biochemical Journal* **283(1)**, 55-61 (1992).

61. McMaster, C.R., Tardi, P.G. & Choy, P.C. Modulation of phosphatidylethanolamine biosynthesis by exogenous ethanolamine and analogues in the hamster heart. *Molecular and cellular biology* **116(1-2)**, 69-73 (1992).

62. Weinhold, P.A. & Rethy, V.B. Separation, purification, and characterization of ethanolamine kinase and choline kinase from rat liver. *Biochemistry* **13(25)**, 5135-5141 (1974).

63. Lasho, T.L. *et al.* Novel recurrent mutations in ethanolamine kinase 1 (ETNK1) gene in systemic mastocytosis with eosinophilia and chronic myelomonocytic leukemia. *Blood cancer journal* **5(1)**, e275-e275 (2015).

64. Van Hellemond, J.J., Slot, J.W., Geelen, M.J., van Golde, L.M. & Vermeulen, P.S. Ultrastructural localization of CTP: phosphoethanolamine cytidylyltransferase in rat liver. *Journal of Biological Chemistry* **269(22)**, 15415-15418 (1994).

65. Bladergroen, B.A. & van Golde, L.M. CTP: phosphoethanolamine cytidylyltransferase. *Biochimica et Biophysica Acta (BBA) - Lipids and Lipid Metabolism* **1348(1-2)**, 91-99 (1997).

66. Fullerton, M.D., Hakimuddin, F. & Bakovic, M. Developmental and metabolic effects of disruption of the mouse CTP: phosphoethanolamine cytidylyltransferase gene (Pcyt2). *Molecular and cellular biology* **27(9)**, 3327-3336 (2007).

67. Vaz, F.d.r.M. *et al.* Mutations in PCYT2 disrupt etherlipid biosynthesis and cause a complex hereditary spastic paraplegia. *Brain* **142(11)**, 3382-3397 (2019).

68. McMaster, C.R. & Bell, R.M. CDP-ethanolamine: 1, 2-diacylglycerol ethanolaminephosphotransferase. *Biochimica et Biophysica Acta (BBA) - Lipids and Lipid Metabolism* **1348(1-2)**, 117-123 (1997).

69. Horibata, Y. *et al.* EPT1 (selenoprotein I) is critical for the neural development and maintenance of plasmalogen in humans. *Journal of Lipid Research* **59(6)**, 1015-1026 (2018).

70. Ahmed, M.Y. *et al.* A mutation of EPT1 (SELENOI) underlies a new disorder of Kennedy pathway phospholipid biosynthesis. *Brain* **140(3)**, 547-554 (2017).

71. Yamamoto, G.L. *et al.* Mutations in PCYT1A Cause Spondylometaphyseal Dysplasia with Cone-Rod Dystrophy. *The American Journal of Human Genetics* **94**, 113-119 (2014).

72. Hollander, A.I.d., Roepman, R., Koenekoop, R.K. & Cremers, F.P.M. Leber congenital amaurosis: Genes, proteins and disease mechanisms. *Progress in retinal and eye research* **27(4)**, 391-419 (2008).

73. Kumaran, N., Moore, A.T., Weleber, R.G. & Michaelides, M. Leber congenital amaurosis/early-onset severe retinal dystrophy: clinical features, molecular genetics and therapeutic interventions. *British journal of ophthalmology* **101(9)**, 1147-1154 (2017).

74. Kara, E. *et al.* Genetic and phenotypic characterization of complex hereditary spastic paraplegia. *Brain* **139(7)**, 1904-1918 (2016).

75. Gietz, D., St. Jean, A., Woods, R.A., & Schiestl, R.H. Improved method for high efficiency transformation of intact yeast cells. *Nucleic Acids Research*. **20(6),** 1425 (1992).

76. Gibellini, F. & Smith, T.K. The Kennedy pathway — de novo synthesis of phosphatidylethanolamine and phosphatidylcholine. *IUBMB life* **62(6)**, 414-428 (2010).

77. Hosaka, K., Tanaka, S., Nikawa, J.-i. & Yamashita, S. Cloning of a human choline kinase cDNA by complementation of the yeast cki mutation. *FEBS letters* **304(2-3)**, 229-232 (1992).

78. Henneberry, A. & McMaster, C. Cloning and expression of a human choline/ethanolaminephosphotransferase: synthesis of phosphatidylcholine and phosphatidylethanolamine. *Biochemical Journal* **339(2)**, 291-298 (1999).

79. Haider, A. *et al.* PCYT1A Regulates Phosphatidylcholine Homeostasis from the Inner Nuclear Membrane in Response to Membrane Stored Curvature Elastic Stress. *Developmental cell* **45(4)**, 481-495 (2018).

80. Henry, S., Gaspar, M. & Jesch, S. The response to inositol: regulation of glycerolipid metabolism and stress response signaling in yeast. *Chemistry and physics of lipids* **180**, 23-43 (2014).

81. Schroeder, L. & Ikui, A. Tryptophan confers resistance to SDS associated cell membrane stress in *Sacharomyces cerevisiae*. *PloS one*. **14(3)**, e0199484 (2019).

82. Pradhan, A., Pinheiro, J.P., Seena, S., Pascoal, C. & Cassio, F. Polyhydroxyfullerene Binds Cadmium Ions and Alleviates Metal-Induced Oxidative Stress in Saccharomyces cerevisiae. *Applied and environmental microbiology* **80**, 5874-5881 (2014).

83. Kodaki, T. & Yamashita, S. Yeast Phosphatidylethanolamine Methylation Pathway. Cloning and characterization of two distinct methylatransferase genes. *Journal of Biological Chemistry*, **262(32)**,15428-15435 (1987).

84. Patton-Vogt, J. *et al.* Role of the Yeast Phosphatidylinositol/Phosphatidylcholine Transfer Protein (Sec14p) in Phosphatidylcholine Turnover andINO1 Regulation. *Journal of Biological Chemistry* **272(33)**, 20873-20883 (1997).

85. Fernández-Murray, J.P. & McMaster, C. Glycerophosphocholine catabolism as a new route for choline formation for phosphatidylcholine synthesis by the Kennedy pathway. *Journal of Biological Chemistry* **280**, 38290-38296 (2005).

86. Fernández-Murray, J.P., Ngo, M.H. & McMaster, C.R. Choline Transport Activity Regulates Phosphatidylcholine Synthesis through Choline Transporter Hnm1 Stability. *Journal of Biological Chemistry* **288(50)**, 36106-36115 (2013).

87. Wakap, S.N. *et al.* Estimating cumulative point prevalence of rare diseases: analysis of the Orphanet database. *European Journal of Human Genetics* **28(2)**, 165-173 (2020).